

Contract No:

This document was prepared in conjunction with work accomplished under Contract No. DE-AC09-08SR22470 with the U.S. Department of Energy (DOE) Office of Environmental Management (EM).

Disclaimer:

This work was prepared under an agreement with and funded by the U.S. Government. Neither the U. S. Government or its employees, nor any of its contractors, subcontractors or their employees, makes any express or implied:

- 1) warranty or assumes any legal liability for the accuracy, completeness, or for the use or results of such use of any information, product, or process disclosed; or
- 2) representation that such use or results of such use would not infringe privately owned rights; or
- 3) endorsement or recommendation of any specifically identified commercial product, process, or service.

Any views and opinions of authors expressed in this work do not necessarily state or reflect those of the United States Government, or its contractors, or subcontractors.

We put science to work.™



**Savannah River
National Laboratory™**

OPERATED BY SAVANNAH RIVER NUCLEAR SOLUTIONS

A U.S. DEPARTMENT OF ENERGY NATIONAL LABORATORY • SAVANNAH RIVER SITE • AIKEN, SC

Thermal Analysis of Saltstone Disposal Units

Si Young Lee

February 2019

SRNL-STI-2019-00015, Revision 0

SRNL.DOE.GOV

DISCLAIMER

This work was prepared under an agreement with and funded by the U.S. Government. Neither the U.S. Government or its employees, nor any of its contractors, subcontractors or their employees, makes any express or implied:

1. warranty or assumes any legal liability for the accuracy, completeness, or for the use or results of such use of any information, product, or process disclosed; or
2. representation that such use or results of such use would not infringe privately owned rights; or
3. endorsement or recommendation of any specifically identified commercial product, process, or service.

Any views and opinions of authors expressed in this work do not necessarily state or reflect those of the United States Government, or its contractors, or subcontractors.

Printed in the United States of America

**Prepared for
U.S. Department of Energy**

Keywords: *Transient Thermal Model,
CFD Model, Hydration Heat*

Retention: *Permanent*

Thermal Analysis of Saltstone Disposal Units

S. Y. Lee

February 2019

Prepared for the U.S. Department of Energy under
contract number DE-AC09-08SR22470.



REVIEWS AND APPROVALS

AUTHORS:

S. Y. Lee, Environmental Modeling Group Date

TECHNICAL REVIEW:

M. R. Kesterson, Tritium Process Science, Reviewed per E7 2.60 Date

APPROVAL:

D. A. Crowley, Manager Date
Environmental Modeling

L. T. Reid, Director, Environmental Restoration Technology Date

T. W. Coffield, Waste Disposal Authority Date

K. H. Rosenberger, Manager Date
Closure & Disposal Assessment

EXECUTIVE SUMMARY

SRR requested that SRNL develop a two-dimensional computer simulation model to be capable of predicting grout temperatures attained in Saltstone Disposal Units (SDUs) during the transient addition of saltstone grout and its subsequent storage period [2]. A simulation model was developed to calculate the transient grout temperatures of the SDU facility by taking an axisymmetric and two-dimensional Computational Fluid Dynamics (CFD) approach. The final performance calculations were based on the conduction and radiation model without a convection cooling mechanism for conservative estimate of the grout temperatures and computational efficiency. While convection within the SDU is disabled in the current calculations, the simulation model has the capability of turning convection back on if desired by the user. Hence, the thermal model in its current configuration is best characterized as a finite-volume heat transfer model. However, given that the model can account for convection if desired by the user, it will be referred to as a CFD model. The grout material contains a transient heat source due to the exothermic hydration reactions of the cementitious material mixed with salt solution. The model can predict the transient temperatures at point locations within the poured grout and the overlying vapor space, and at the interior and exterior surfaces of the structure.

The thermal model has been developed for two SDUs at the Savannah River Site (SRS); namely, SDU 2A and SDU 6. SDU 2A is a cylindrical unit measuring 150 feet (ft) in diameter, 22 ft tall, and holds approximately three million gallons of grout. SDU 6 is 375 ft in diameter and 43 ft high with a capacity of over thirty million gallons. Prior to performing the thermal calculations for the SDU 6 facility, the benchmarking test for the smaller SDU 2A unit was performed to establish the solution method and to verify the computational results using existing thermocouple data. Based on the Lagrangian discrete method and boundary conditions established by the SDU 2A benchmarking test, the CFD calculations were performed to predict the transient temperatures at local positions of the poured grout and air spaces within the SDU 6 structure.

From the SDU 2A benchmarking results, it is noted that when the grout level exceeds the approximate height of 17 ft, the model underestimates grout temperatures by about 4°C; this was associated with short idling periods (i.e., no grout addition to the SDU), and is potentially due to the uneven nature of the grout accumulation in the SDU (in comparison to the uniform grout layering in the model), or variations in the saltstone formulation associated with variable raw materials and salt solution composition. Comparing the transient behaviors of the predicted grout temperatures with the SDU thermocouple data, it is concluded that the SDU 2A model provides a conservative prediction with respect to the maximum grout temperatures. In addition, it was confirmed that the computer model overpredicted the maximum grout temperatures in SDU 2A by approximately 10°C. Furthermore, the peak predicted temperature reached by the saltstone is far below the maximum allowable temperature, which is 95°C saltstone temperature per Documented Safety Analysis of the saltstone facility [1].

Based on the solution method and modeling boundary conditions verified by the SDU 2A benchmarking tests, the SDU 6 model was developed for a quantitative assessment of the transient temperatures at point locations within the grout associated with a pour schedule having 12.3 days of continuous pouring followed by 46.6 days of idling time. The modeling results show that when the pouring was started in January, a maximum grout temperature of ~52°C was reached at the end of pouring. The model developed in this study will be used to predict grout temperatures within an SDU for different saltstone pour schedules, SDU designs, and saltstone compositions (with varied thermal properties).

TABLE OF CONTENTS

LIST OF TABLES	vii
LIST OF FIGURES	vii
LIST OF ABBREVIATIONS and NOMENCLATURE	ix
1.0 Introduction.....	1
2.0 Modeling Geometry and Solution Methodology	3
2.1 Solution Approach and Governing Equations.....	6
2.2 Modeling Domain Size and Boundary Conditions.....	11
2.3 Hydration Heat Source of Grout Material	18
2.4 Ambient temperature and solar heat around the SDU.....	19
2.5 Grout Pouring Schedule of SDU facility.....	22
2.6 Discretization of Modeling Domain.....	23
3.0 Benchmarking Test for SDU 2A.....	27
4.0 Results and Discussion	33
5.0 Conclusions.....	36
6.0 References.....	38
Appendix A . Transient Thermal Source and Grout Pour Schedule	A-1
Appendix B . Computer Input Files for Ambient Temperature and Hydration Heat Source.....	B-26

LIST OF TABLES

Table 2-1. Material and thermal properties of SDU components as used for the thermal calculations.....	9
Table 2-2. Domain size and boundary conditions for SDU thermal model.....	17
Table 2-3. Solar heat for the SDU facility	22

LIST OF FIGURES

Figure 1-1. Geometrical configurations and modeling domain of the SDU 2A for the thermal modeling analysis (noting that the roof support columns are not included in the model) [3].....	2
Figure 1-2. Geometrical configurations and modeling domain of the SDU 6 (as modeled for the thermal performance analysis) [6].....	3
Figure 2-1. Axisymmetric two-dimensional modeling domain of SDU 2A facility.....	4
Figure 2-2. Modeling calculations and benchmarking tests of SDU 2A model	5
Figure 2-3. Thermal conductivity of air containing 50% relative humidity as function of ambient temperatures for the present calculations.	10
Figure 2-4. Thermal capacities of air and vapor as function of temperature.	11
Figure 2-5. Evaluation of the soil width on the computational results	12
Figure 2-6. Evaluation of the soil conductivity on the computational results.....	13
Figure 2-7. Evaluation of ambient air temperature on the computational results	14
Figure 2-8. Convective cooling mode for a thermal boundary layer established by wind speed V_w on the top external surface of SDU 2A modeling domain as used for the thermal calculations.....	15
Figure 2-9. Heat transfer coefficients as function of ambient wind speed.....	16
Figure 2-10. Temperature distributions along the vertical centerline	17
Figure 2-11. Comparison of hydration heat sources between the two different SDU grout formulations..	19
Figure 2-12. Ambient temperatures for SDU 2A between August 9, 2012 and June 30, 2014.....	20
Figure 2-13. Ambient temperatures for SDU 6 during a five-month period of January to July.	21
Figure 2-14. Transient grout height above the SDU 2A floor during the grout pouring period.	24
Figure 2-15. Transient grout height above the SDU 2A floor during the active filling period of August 10, 2012 to June 11, 2014.....	24
Figure 2-16. Transient grout heights above the SDU 6 floor during the grout pouring period.	25
Figure 2-17. Two-dimensional computational meshed for SDU 2A modeling domain as used for the thermal benchmarking calculations.....	26

Figure 2-18. Two-dimensional computational meshes for the axisymmetric modeling domain of SDU 6 as used for the thermal performance calculations..... 26

Figure 3-1. Thermocouple locations for the SDU 2A facility. 28

Figure 3-2. Comparison of the modeling predictions and SDU 2A thermocouple data for the grout height less than 3.5 ft..... 29

Figure 3-3. Comparison of the modeling predictions and SDU 2A thermocouple data at the thermocouple position 2.5 ft for Train A/B..... 30

Figure 3-4. Comparison of the modeling predictions and SDU 2A thermocouple data at the thermocouple position 10.5 ft for Train A/B..... 31

Figure 3-5. Comparison of maximum grout temperatures between the modeling predictions and SDU 2A thermocouple data at the completion of pouring 32

Figure 3-6. Comparison of transient SDU 2A thermocouple data at position 10.5 ft..... 33

Figure 4-1. Modeling predictions for the SDU 6 facility for the operation schedule of 12.3 days pouring and 46.6 days' idle..... 35

Figure 4-2. Transient temperature profiles along the vertical centerline of the SDU 6 facility..... 36

LIST OF ABBREVIATIONS and NOMENCLATURE

CFD	Computational Fluid Dynamics
SDU	Saltstone Disposal Unit
SRNL	Savannah River National Laboratory
SRR	Savannah River Remediation
SRS	Savannah River Site
'	foot (length)
"	inch (length)
atm	Atmospheric pressure unit
C_p	Specific heat
ft	feet
g	Gravitational acceleration (m/sec ²)
gpm	Gallons per minute
h_w	Wall heat transfer coefficient
Δh	Grout height increment
k	Thermal conductivity
p	Air pressure
\bar{q}_{cond}	Conductive heat transfer rate per unit area (W/m ²)
\bar{q}_{rad}	Radiative heat transfer rate per unit area (W/m ²)
T	Temperature
t	Time
Δt	Time difference
v	Velocity
r	Radial coordinate
z	Axial coordinate
ρ	Density
τ	Normal or shear stress
X	Gravity force per unit volume

1.0 Introduction

The Saltstone Disposal Units (SDUs) are utilized for the permanent storage of low-level activity waste grout, termed saltstone, produced from the solidification of decontaminated salt waste at the Savannah River Site (SRS). These units are cylindrical concrete tanks that are based on a design used commercially for liquid storage. The present work is focused on the thermal modeling analysis of the SRS disposal units: SDU 2A and SDU 6. As shown in Fig. 1-1, SDU 2A is cylindrical tank that is 150 feet (ft) in diameter, 22 ft tall, and holds approximately three million gallons of saltstone grout. The SDU 6 is a larger scale unit of 375 ft in diameter and 43 ft high with a capacity over thirty million gallons as shown in Fig. 1-2. The hydration process of the grout material produces thermal heat from an exothermic chemical reaction. Due to the concern of the flammable gas generation by organic materials present in the saltstone waste form, it is necessary to keep the grout temperature below 95°C [1]. In this work, several different types of scoping analyses were performed to define the optimal modeling domain boundary including parametric sensitivity calculations of soil thickness and soil conductivity.

The primary goal of the project is to develop a Computational Fluid Dynamics (CFD) simulation model capable of predicting temperatures in the SDUs attained initially during the addition of grout (i.e., a hydrating cementitious material containing a heat generation source), and subsequently during the post-pour storage phase. The model shall have the capability to predict the transient temperatures at point locations within the poured grout, the overlying vapor spaces, and the interior/ exterior surfaces of the SDU as shown in Fig. 1-1. The model developed in this study will be used to predict grout temperatures within an SDU for different saltstone pour schedules, SDU designs, and saltstone compositions (with varied thermal properties).

As requested by SRR, the main objectives of the present work are to [2]:

- Develop a computational model to predict temperatures reached in SDU 2A during the saltstone grout addition and its subsequent storage period.
- Benchmark the modeling predictions against grout temperature data measured in SDU 2A.
- Perform a sensitivity analysis with respect to the baseline design and operating conditions such as grout pour schedule and seasonal and ambient conditions.
- Create a large-scale model of SDU 6 based on the modeling parameters established by the SDU 2A benchmarking test results.

The work considers two different disposal units: SDU 2A and SDU 6. Prior to performing the thermal calculations for the SDU 6 facility, the benchmarking test for the SDU 2A unit was performed to establish the solution method and to verify the computational modeling predictions using the SDU 2A thermocouple data. Based on the solution method and the boundary conditions established by the SDU 2A benchmarking test, the CFD calculations were performed to predict the maximum temperatures of the poured grout within the SDU 6 structure.

A CFD modeling approach was taken to achieve the objectives. Based on the modeling domains of SDU 2A and SDU 6, as defined in Figure 1-1 and Figure 1-2, a transient axisymmetric two-dimensional approach was taken to compute component temperatures for the SDU domains by using a commercial CFD software, ANSYS-FLUENT™.

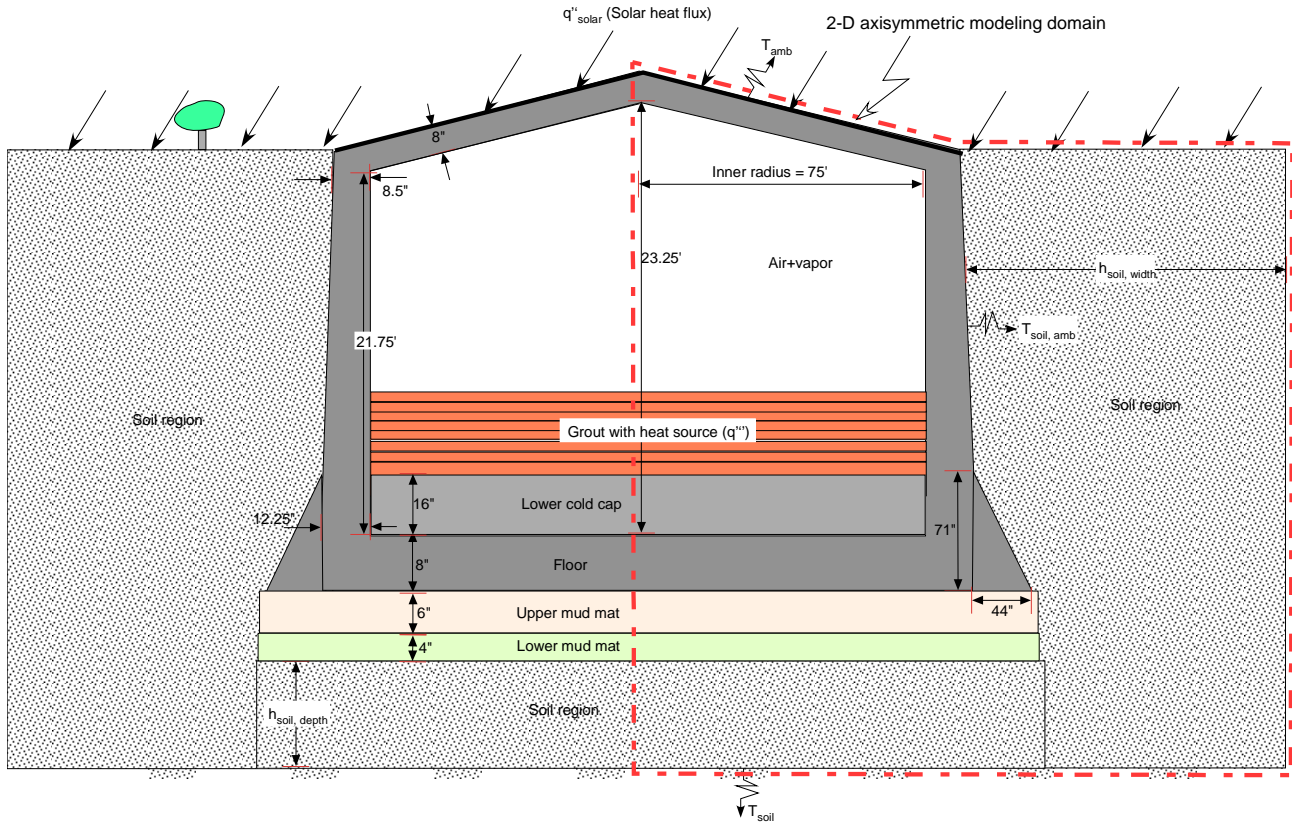
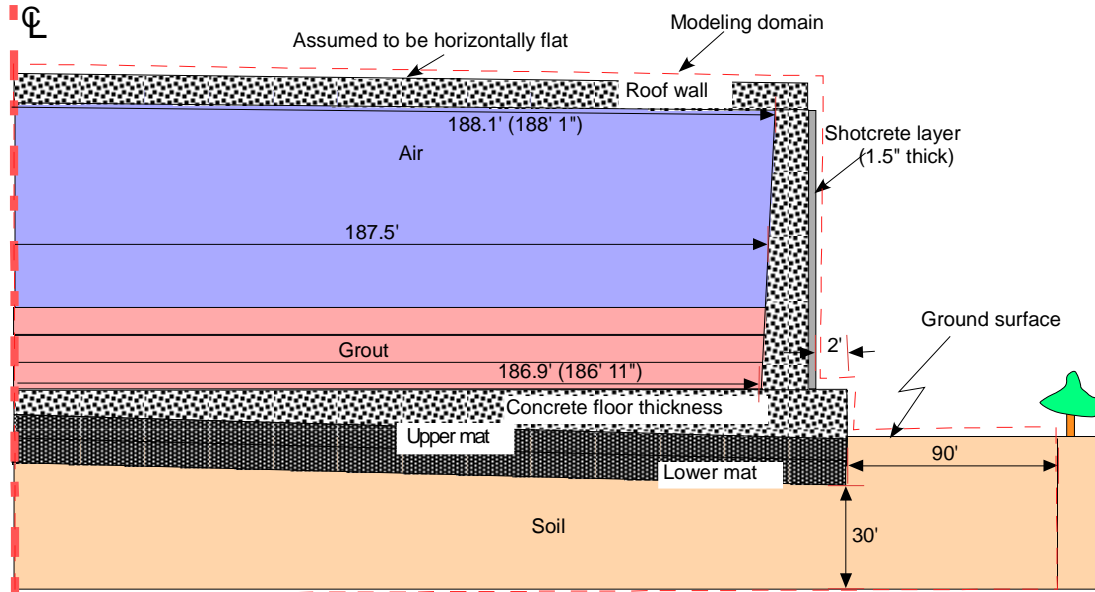


Figure 1-1. Geometrical configurations and modeling domain of the SDU 2A for the thermal modeling analysis (noting that the roof support columns are not included in the model) [3].



Detailed component dimensions for SDU 6:

Concrete floor wall thickness = 1' to 2'; Roof wall thickness = 1' ; SDU side wall thickness = 10" to 24" ; SDU side inner height = 43' ; SDU center inner height = 43'; Upper mat thickness = 6"; Lower mat thickness = 4"

Figure 1-2. Geometrical configurations and modeling domain of the SDU 6 (as modeled for the thermal performance analysis) [6].

2.0 Modeling Geometry and Solution Methodology

The modeling geometry was based on the prototypic dimensions and configurations as shown in Figure 2-1, and it was developed on a LINUX computing platform. As shown in Figure 2-2, the basic solution method was based on a transient CFD model combined with Lagrangian discrete source regions for computational efficiency. In this method, the predetermined air region is replaced by a grout material with hydration heat source as the grout material is progressively accumulated on the SDU floor. The accumulation rate of grout is, of course, dependent on the pour schedule. The air region replaced by grout represents the grout layer accumulated from an SDU pouring schedule. The grout region has a transient heat source term that is generated by the exothermic chemical hydration reaction, and the source term is quantified by experimental work [4]. At the beginning of each pour, a grout layer predetermined by the pouring time was modeled to have a transient heat source corresponding to the middle of the pouring hours.

The benchmarking tests were conducted for SDU 2A. When hydration heat sources (provided by Savannah River Remediation LLC (SRR)) and ambient temperature data (measured at the Savannah River National Laboratory (SRNL)) are input into the SDU 2A CFD model, the transient modeling predictions were benchmarked against the thermocouple data obtained during a period of approximately 16,000 hours from August 2012 to June 2014. Based on the modeling parameters established by the SDU 2A benchmarking test results, a model of the SDU 6 facility (2.5 times larger than SDU 2A in diameter) was developed to predict the transient temperatures at point locations within the poured grout, the overlying vapor space, and the interior/exterior surfaces of the SDU structure (as shown in Figure 1-2). The model developed in this study will be used to predict grout temperatures within an SDU for different saltstone pour schedules, SDU designs, and saltstone compositions (with varied thermal properties). The descriptions of the solution

method used here are graphically presented in Figure 2-2, and detailed discussions are provided in the subsequent section.

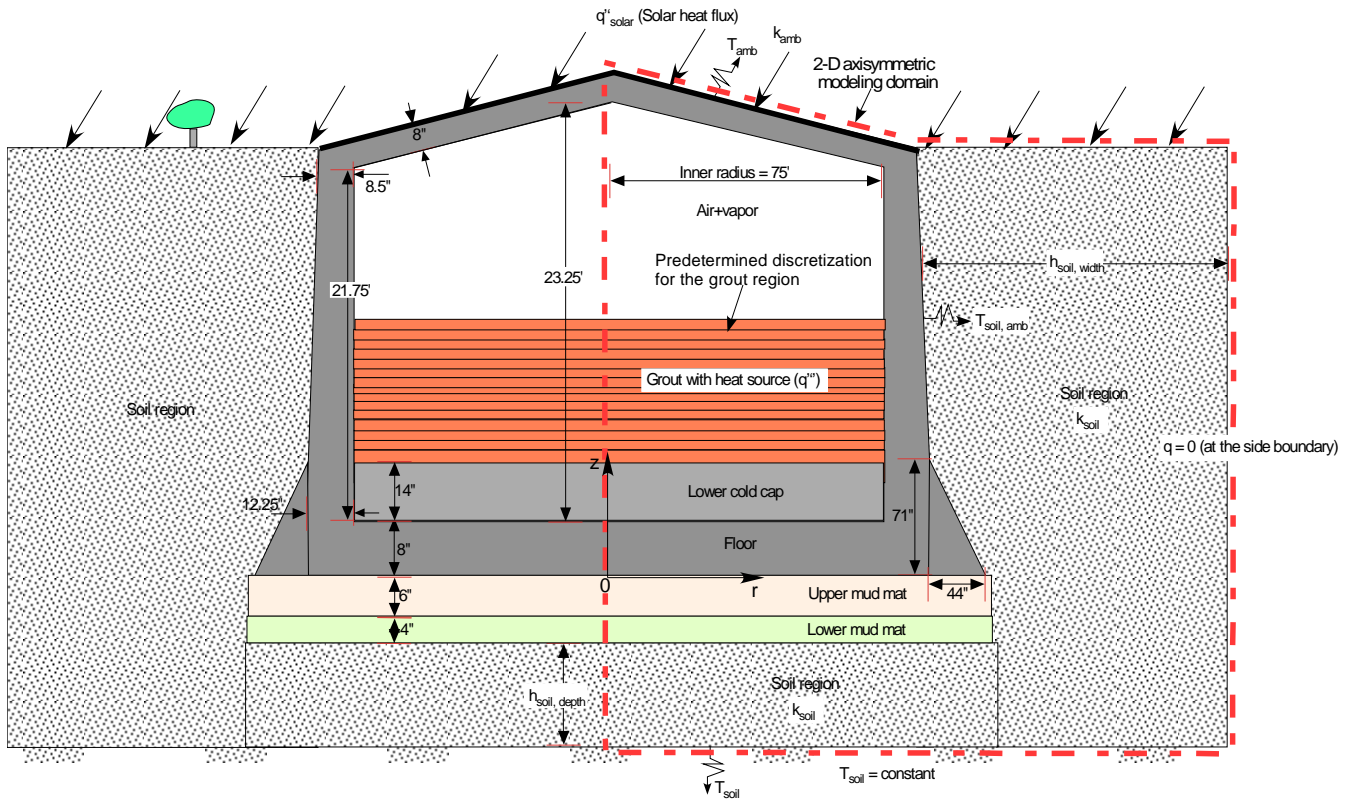


Figure 2-1. Axisymmetric two-dimensional modeling domain of SDU 2A facility

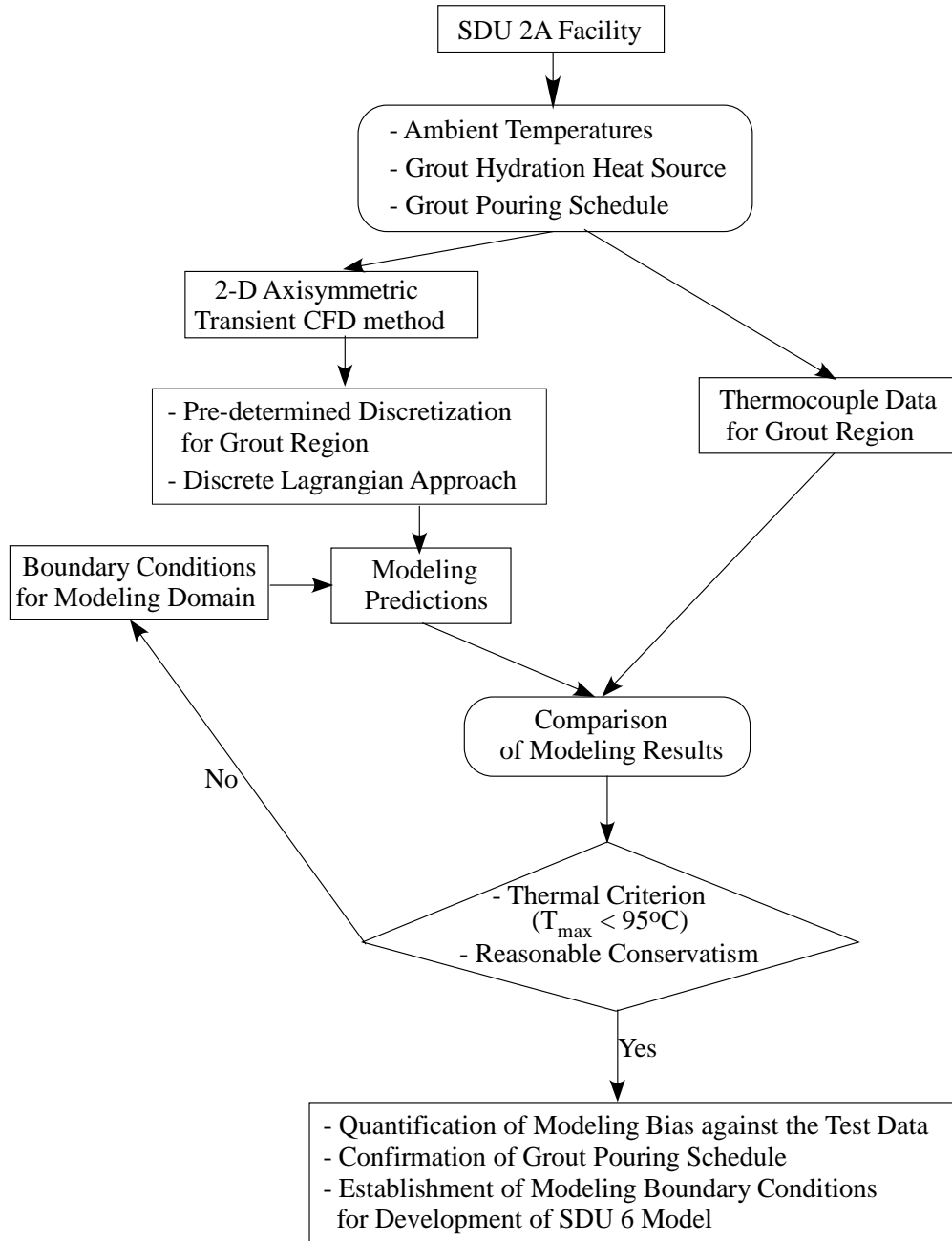


Figure 2-2. Modeling calculations and benchmarking tests of SDU 2A model

2.1 Solution Approach and Governing Equations

The main objective of this work was to develop a computational model to predict the time-dependent temperatures attained within a grout material (in an SDU) during the periods of initial addition of grout and subsequent storage. To achieve the objective, a transient two-dimensional CFD modeling approach was used for the thermal calculations of the SDU grout materials by using a conduction-convection cooling mechanism coupled with radiation. Benchmarking analysis for SDU 2A, and the main performance calculations for SDU 6, were made using the conduction-radiation cooling mode due to its computational efficiency and conservative assessment. The geometrical configurations for the modeling domains for SDU 2A and SDU 6 are shown in Figures 1-1 and 1-2, respectively. The modeling simulations used two-dimensional transient governing equations with axisymmetry assumptions. For the SDU thermal analysis, a transient thermal load (determined by the grout pouring schedule) was assumed to be primarily cooled by a coupled conduction and radiation mechanism for the modeling domain defined by the boundary conditions. The boundary conditions such as ambient conditions and geological domain size around the SDU system are subsequently discussed.

The basic equations governing the thermal energy transport must be coupled with those of fluid motion in order to describe, mathematically, the process of energy transfer for an SDU modeling domain. Thus, a computational model considers heat transfer mechanisms driven by convection and radiation as well as conduction for the vapor space enclosed in the SDU. Temperature decreases rapidly due to the convective and radiative cooling effects within a boundary layer region adjacent to the wall surface, as provided in the literature [7,13]. The boundary layer flow is a buoyancy-induced motion resulting from body forces acting on density gradients which, in turn, arise from temperature gradients in the vapor space of the SDU. It is virtually impossible to observe pure heat conduction in a gas medium because as soon as a temperature difference across the interface of grout wall and vapor gas inside an enclosed SDU is imposed on the gas, natural convection currents occur as a result of density differences. In this case, it is noted that if an SDU model containing a transient heat source does not consider a convective cooling mechanism due to the buoyant gas motion, the predicted grout temperature may be higher than in reality because of a reduced thermal dissipation of the grout heat into the soil and ambient air. However, a temperature change due to the neglect of the natural convection is expected to be small because of the low range of the SDU temperatures considered here. The relative importance of the different grout cooling mechanisms was not explicitly assessed.

When natural convection due to the air temperature differences is considered for the enclosed air space above the grout layer of the SDU, a full set of mathematical equations can be provided that govern the transient heat transfer problem over the modeling domain of the SDU under the axisymmetrically two-dimensional cylindrical coordinate system.

For the mass continuity,

$$\frac{\partial \rho}{\partial t} + \frac{1}{r} \frac{\partial}{\partial r} (\rho r v_r) + \frac{\partial}{\partial z} (\rho v_z) = 0 \quad (1)$$

For the momentum balance equations with a shear stress τ along the radial r-direction and axial z-direction of the cylindrical coordinate system,

$$\rho \left(\frac{\partial v_r}{\partial t} + v_r \frac{\partial v_r}{\partial r} + v_z \frac{\partial v_r}{\partial z} \right) = - \frac{\partial p}{\partial r} - \left(\frac{1}{r} \frac{\partial (r \tau_{rr})}{\partial r} + \frac{\partial (\tau_{rz})}{\partial z} \right) + X_r \quad (2)$$

$$\rho \left(\frac{\partial v_z}{\partial t} + v_r \frac{\partial v_z}{\partial r} + v_z \frac{\partial v_z}{\partial z} \right) = - \frac{\partial p}{\partial z} - \left(\frac{1}{r} \frac{\partial (r \tau_{rz})}{\partial r} + \frac{\partial (\tau_{zz})}{\partial z} \right) + X_z \quad (3)$$

The first terms on the Left-Hand Side (LHS) in Equations (2) and (3) are transient momentums per unit volume. The second and third terms on the LHS of the equations are rate of momentum increases per unit volume, and the first and second terms on the Right-Hand Side (RHS) of Equations (2) and (3) represent pressure and shear stress forces per unit volume along the radial and axial directions, respectively. The parameter, τ_{rr} , in the equations is normal stress on the r-face, and τ_{rz} the axial z-directed shear (or tangential) stress on the r-face resulting from viscous forces. All the parameters of the momentum equations are defined in the Nomenclature section. For the present modeling domain, as shown in Figures 1-1 and 1-2, the gravity forces per unit volume along the horizontal r-coordinate are zero, $X_r = 0$, and the gravitational term of the momentum equation along the vertical z-coordinate, X_z , is used to include buoyancy-induced natural convection. The work neglects all variable property effects due to temperature changes in the governing equations except for air. The thermal conductivity of air is considered to be dependent on temperature, and air density is approximated as an ideal gas under 1 atm. ambient pressure. The gravity term in the z direction in Equation (3), $X_z = -\rho g$.

When the conduction, convection, and radiation heat transfer mechanisms are applied for the evaluation of the thermal performance in the SDU, a transient thermal energy balance equation (under the axisymmetrical and cylindrical coordinate system) can be defined as follows:

$$\rho C_p \left(\frac{\partial T}{\partial t} + v_r \frac{\partial T}{\partial r} + v_z \frac{\partial T}{\partial z} \right) + \nabla \cdot (\bar{q}_{cond} + \bar{q}_{rad}) - \dot{q}'' = 0 \quad (4)$$

The first term in LHS of Equation (4) represents transient thermal response. The second and third terms in Equation (4) are the natural convective terms derived by local air velocities (v_r and v_z) due to the temperature gradient inside the SDU; assuming an enclosed air that follows ideal gas behavior. \bar{q}_{cond} in the energy balance represents conductive heat flux, and the radiation heat flux term, \bar{q}_{rad} , in the equation was calculated by the discrete ordinate method [12]. The last term of the equation is a volumetric heat source generated within the modeling domain. In this work, the heat source predominantly results from the hydration reactions of the grout material, which are provided by the modeling input.

For the present analysis, the convection term was not considered when the SDU air space was assumed to be completely frozen and conductively controlled for a conservative assessment of grout temperatures. As a result of this assumption, the computational time was significantly reduced. Therefore, the present calculations were only conducted for the thermal energy balance, Equation (4), without considering the momentum balance and mass continuity equations. The heat source term, \dot{q}'' , is included in the energy equation, Equation (4), as a model input. Complete setup of the modeling calculations required input parameters, such as the thermal and material properties of the SDU materials of construction, the heat source term, boundary conditions, and domain discretization, along with the established modeling domain and assumptions. These are subsequently discussed.

Modeling calculations were based on the following assumptions:

- The prototypic structure of the SDU facility is approximated to be symmetrical along the vertical centerline for computational efficiency.
- The initial temperature for the interior region of the SDU is assumed to be uniform (26.85°C).
- The vapor space above the grout region is initially stagnant.
- Air is assumed to follow ideal gas behavior.

- Although the thermal model was originally developed by considering a conduction-convection cooling mechanism coupled with radiation, the current calculations do not include convection cooling for conservative assessment and computational efficiency.
- Any movement in the grout region during the grout filling period is assumed to be frozen so that conduction and radiation are dominant as the primary cooling mechanism.
- Transient thermal calculations are based on a completely enclosed SDU boundary; the internal air of the SDU facility has no flow communication with external ambient air through the SDU wall boundary.
- Obstruction effects on thermal transport in the vapor space of the SDU are assumed to be negligible: i.e., 48 roof support columns, each column 14-in. in diameter were not considered in the SDU 2A thermal calculations. Additionally, it should be noted that the roof support columns present in SDU 6 were not considered in the SDU 6 thermal calculations either.
- Condensation effects of vapor inside the free space above the grout region is neglected.
- The grout layer has an evenly distributed hydration heat.
- The top grout surface is horizontally flat.
- The 24-hour average insolation heat is always applied to the external surface boundary of the SDU facility, regardless of the weather or time of day.
- During a pouring period, a transient accumulation of grout material on the SDU floor is considered with the discrete Lagrangian approach; this maintains tracking of the transient history of grout aging with respect to the time-dependent hydration heat of the grout.
- The initial grout volume is based on the cold cap region of a 16-in. height on the SDU floor, but the cap region does not contain the hydration heat source.

Neglecting the thermal impact on the grout layer along the azimuthal direction, the calculations were based on an axisymmetrical two-dimensional approach to simplify the solution method for a large modeling domain of the SDU facility because, at a given elevation above the SDU floor, the thermocouple data show that the grout temperature difference azimuthally is less than a few degrees. The model assumed the grout layer to be accumulated on the SDU floor in radially flat and uniform way. In case of nonuniform formation of the grout layer, the grout region may have a local temperature spike due possibly to uneven height or non-uniform composition of the grout layer with trapped air pockets. In addition, the current model does not consider the conduction paths due to the presence of interior concrete support columns. Neglecting these conduction paths will provide a conservative estimate of the grout temperature. For this work, the condensation effect of vapor gas mixed with air inside the SDU was not considered for a conservative thermal assessment because the heat loss resulting from the phase change of the condensable vapor to water droplet was not included in the energy balance calculation of the SDU domain.

The thermal and material properties of the SDU components are shown in Table 2-1. The SDU 2A grout shown in this table is identical to the “H45-45-10” saltstone simulant prepared using “Tank 50 CY2013 Q1-Q3” salt waste simulant presented in Table 1 and Figure 8 of the reference [20]. The SDU 6 grout shown in Table 2-1 is identical to the cement-free “L60-40” saltstone simulant prepared using “New SWPF” salt waste simulant presented in Table 1 and Figure 8 of the reference [20].

Table 2-1. Material and thermal properties of SDU components (as used for the thermal calculations)

Materials	Density Kg/m ³	Specific heat J/kg-K	Thermal conductivity W/m-K	Emissivity [15]
Air [15]	0.998	1009	0.03	
SDU 2A grout*	1710	1940	0.8	0.9
SDU 6 grout*	1710	1960	0.74	0.9
Concrete [16]	2250	1000	1.7	0.9
Soil**	1940	1141.5	1.985	0.9

Note: * Nominal averaged value [4]

** Averaged value [9]

The empty space above the top surface of the poured grout is occupied by humid air consisting of air and water vapor. An adequate description of the thermodynamic state for the air-vapor-mixture system in the air space of the SDU facility can be provided by assuming the gas mixture follows perfect-gas behavior, and Dalton's Law with respect to the air and vapor pressure as a function of temperature. The mixture relationships are based on the definitions of the quantities involved as follows:

Mole fraction, X_v , of the component vapor in the mixture:

$$X_v = m_v \left(\frac{X_v M_v + X_{air} M_{air}}{M_v} \right) \quad (5)$$

In Equation (5) M_v and M_{air} are the molecular weights for vapor and air, respectively. When gas mole fractions, X_v and X_{air} , for the vapor and air species contained in the SDU space are known, the mass fraction, m_v , of the vapor gas component in the gas mixture can be calculated by Equation (6).

$$m_v = \left(\frac{X_v M_v}{X_v M_v + X_{air} M_{air}} \right) \quad (6)$$

The following relation between the mole fraction and the partial pressure for the vapor exists for a perfect-gas mixture:

$$X_v = \left(\frac{P_v}{P_{amb}} \right) \quad (7)$$

In Equation (7) P_{amb} and P_v , are the ambient total pressure of the SDU space and the partial pressure of the vapor gas, respectively. The partial pressure P_v can be determined using the Relative Humidity (RH), ϕ , which is the ratio of P_v to P_{sat} . For an air-vapor mixture, the mass fraction, m_v , for vapor gas can be obtained in terms of vapor partial pressure and molecular weight ratio of the two gases from Equations (6) and (7).

$$m_v = \left(\frac{\phi P_{sat}}{1.61 P_{amb} - 0.61 \phi P_{sat}} \right) \quad (8)$$

P_{sat} in Equation (8) is calculated by the equation correlated in terms of local temperature, and 1.61 is the ratio of air to vapor molecular weights. Thermal and material properties for the humid air (with 50% RH) were estimated in terms of mass fraction, m_v , assuming the vapor and dry air were homogeneously mixed. All the detailed correlations for vapor and dry air are provided in the literature [15]. The thermal and material properties for dry air and 50% RH air (under the potential range of the SDU air temperatures) are compared in Figures 2-3 and 2-4. As shown in these figures, the thermal conductivity of dry air is about 25% higher than that of vapor for the potential range of SDU indoor temperatures; however, the thermal capacity of the dry air is about 16% lower than pure water vapor. Due to these counteracting physical behaviors, it is anticipated that when the grout hydration heat is cooled by a back-filled gas such as air, the time to reach a certain temperature of the grout surface will not be sensitive to the relative humidity. Thus, the thermal properties for regular dry air were used for the modeling analysis of the SDU.

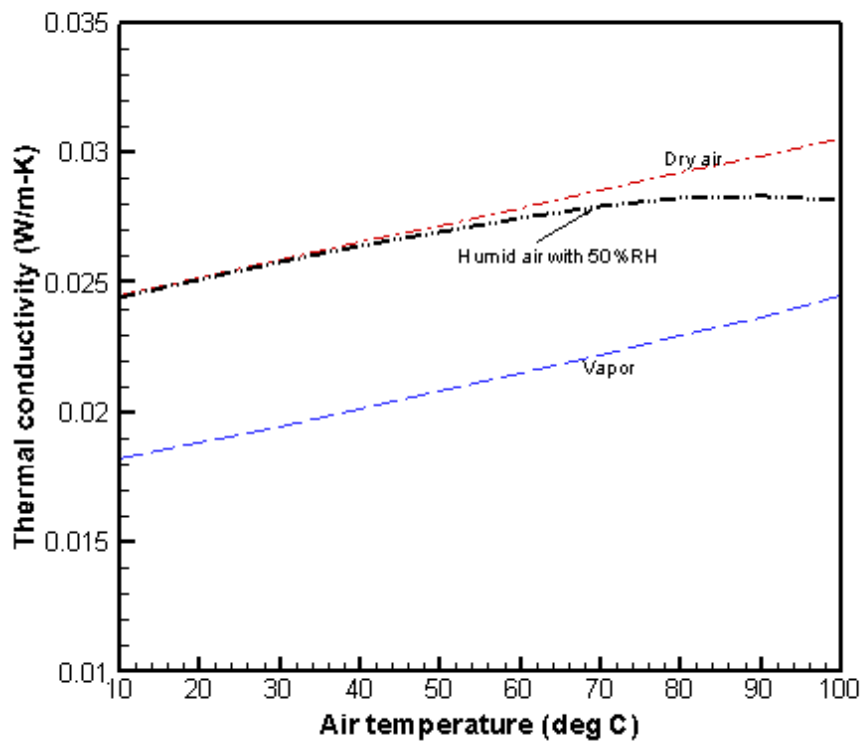


Figure 2-3. Thermal conductivity of air containing 50% relative humidity as function of ambient temperatures for the present calculations.

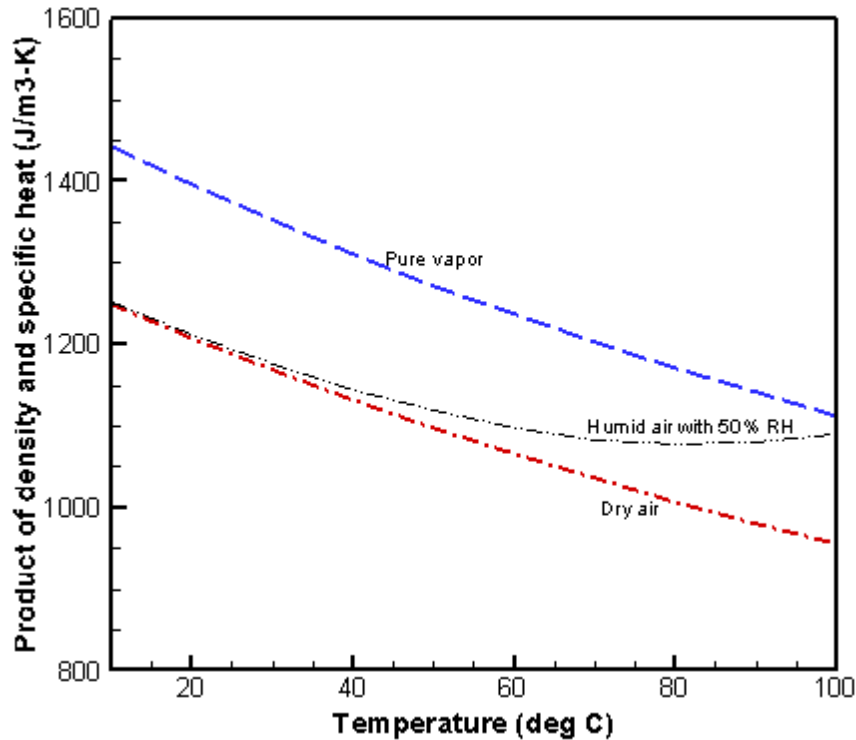


Figure 2-4. Thermal capacities of air and vapor as function of temperature.

2.2 Modeling Domain Size and Boundary Conditions

The modeling domain and component regions used for the thermal calculations are shown in Figure 2-1, and the thermal properties for the components are shown in Table 2-1. The sensitivity calculations were performed to determine the optimum domain boundary. The sensitivity calculations have been made by a cooling mechanism of conduction and radiation as used in the benchmarking test. The sensitivity analysis was focused on the SDU 2A domain because the difference of the domain boundaries between the two units of SDU 2A and SDU 6 is basically at their side wall boundaries: soil-cooled boundary for SDU 2A vs. air-cooled boundary for SDU 6. Thus, there is no need for the sensitivity analysis to determine the optimal domain size beyond the side wall of the SDU 6 model because the side boundary is exposed to the ambient air, and it is provided as one of the modeling boundary conditions.

The nomenclature shown in Figure 2-1 includes a series of parametric calculations for horizontal soil depth below the SDU bottom boundary ($h_{\text{soil,depth}}$), horizontal soil width beyond the SDU side boundary ($h_{\text{soil,width}}$), soil thermal conductivity, and ambient temperature. The soil depth was determined by assuming that the groundwater table acts as an infinite heat sink, and that it maintains a constant temperature. The location of the groundwater region near the SRS SDU facility was obtained from the SRS Environmental Restoration Data Management System (ERDMS: <http://www.srs.gov/deidms/index.html>). From the ERDMS database, the nominal depth ranges 50 to 60 ft. below the ground surface, resulting in average depth of 55 ft. below the ground surface. The corresponding depth below the SDU facility, $h_{\text{soil,depth}}$, is approximately 30 ft. The measured temperature at the groundwater table was 17.4 °C. Thus, the boundary conditions at the domain

bottom were defined as 30 ft. of $h_{\text{soil,depth}}$ and 17.4°C temperature. The ranges of the other sensitivity parameters considered here are:

- Soil thickness ($h_{\text{soil,width}}$): varied from 30 ft. to 270 ft. for a given soil depth.
- Soil thermal conductivity (k_{soil}): varied from 0.25 to 3.72 W/m-K.
- Ambient Temperature Sensitivity (T_{amb}): varied from 70°F (21°C) to 110°F (43°C).

For the sensitivity calculations, a steady state model was applied to the SDU 2A modeling domain of Figure 1-1 with a 30ft. soil depth. The SDU domain has 20 ft. of grout material on the SDU floor containing a volumetric heat source of 1 W/m³. The temperature of the bottom of the soil region was set to 17.4°C. The soil sides are set to be adiabatic. Ambient temperature was set to 100°F. The heat flux from the SDU roof and the earth’s surface is 163.2 W/m² [10]. For this analysis, the SDU roof exposed to the ambient conditions was assumed to be cooled by natural convection. For this case, a typical convective heat transfer coefficient at the external wall boundary (h_w) is 1.5 W/m²-K [11,13].

Domain Size of Soil Region ($h_{\text{soil,width}}$): for a given soil depth, a range of different soil width along the horizontal direction beyond the SDU side wall were considered to evaluate the thermal impact of maximum grout temperatures on the soil domain size surrounding the SDU facility. As shown in Figure 2-5, the calculation results show that when the size is larger than 90 ft. from the SDU side wall boundary, the maximum grout temperature is not sensitive to the horizontal soil thickness $h_{\text{soil,width}}$.

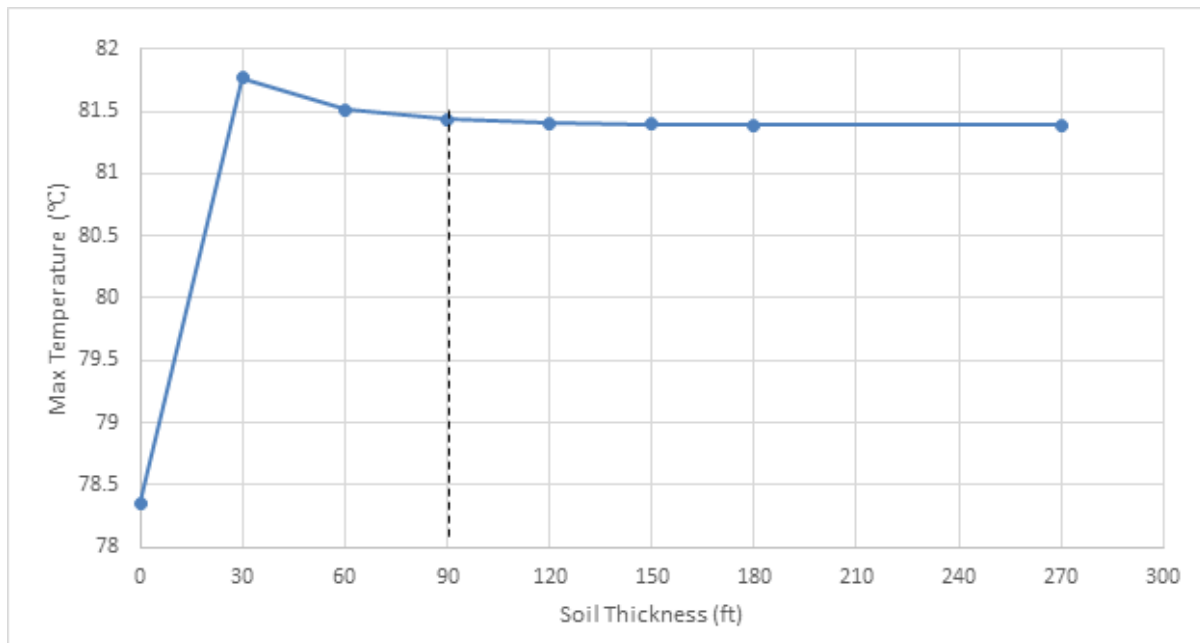


Figure 2-5. Evaluation of the soil width on the computational results

Soil Thermal Conductivity (k_{soil}): based on the established modeling conditions as discussed earlier, a series of sensitivity calculations for different soil thermal conductivities was performed to evaluate the thermal impacts of various soil thermal properties on the SDU facility. A sensitivity analysis for different soil thermal properties with respect to the nominal case of half-saturated soil was performed to determine the impact the soil thermal conductivity on the grout temperature. Soil thermal conductivities can vary from 0.25 to 3.72 W/m-K, depending on the moisture of the soil. As shown in Figure 2-6, the results show that the thermal conductivity of dry sand (0.25 W/m-K [9]) would raise the max temperature by 14°C compared

to wetter soil at a thermal conductivity of 2 W/m-K. Based on this assessment, a median value of the range of the soil thermal conductivities, 1.985 W/m-K, was used for the SDU thermal calculations as shown in Table 2-1.

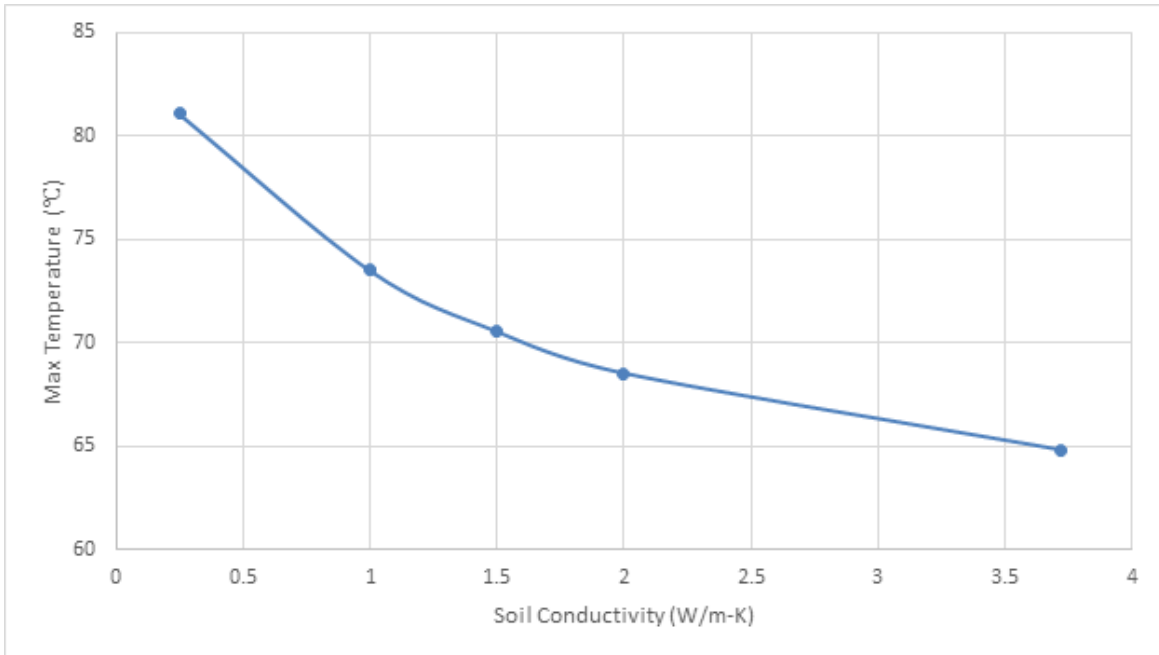


Figure 2-6. Evaluation of the soil conductivity on the computational results

Ambient Temperature (T_{amb}): Sensitivity analysis for different ambient temperatures was performed for the assessment of the thermal impact on the SDU grout temperature under steady state conditions. The average air temperatures surrounding the SDUs typically range 35°C to 38°C during the hotter summer months. As seen in Figure 2-7, the steady state calculation results show that the ambient temperature has a linear effect on the max temperature of the SDU grout as expected. The results show that when ambient temperature increases from 25°C to 35°C, the maximum grout temperature is increased by about 8°C. The corresponding slope is approximately 0.8.

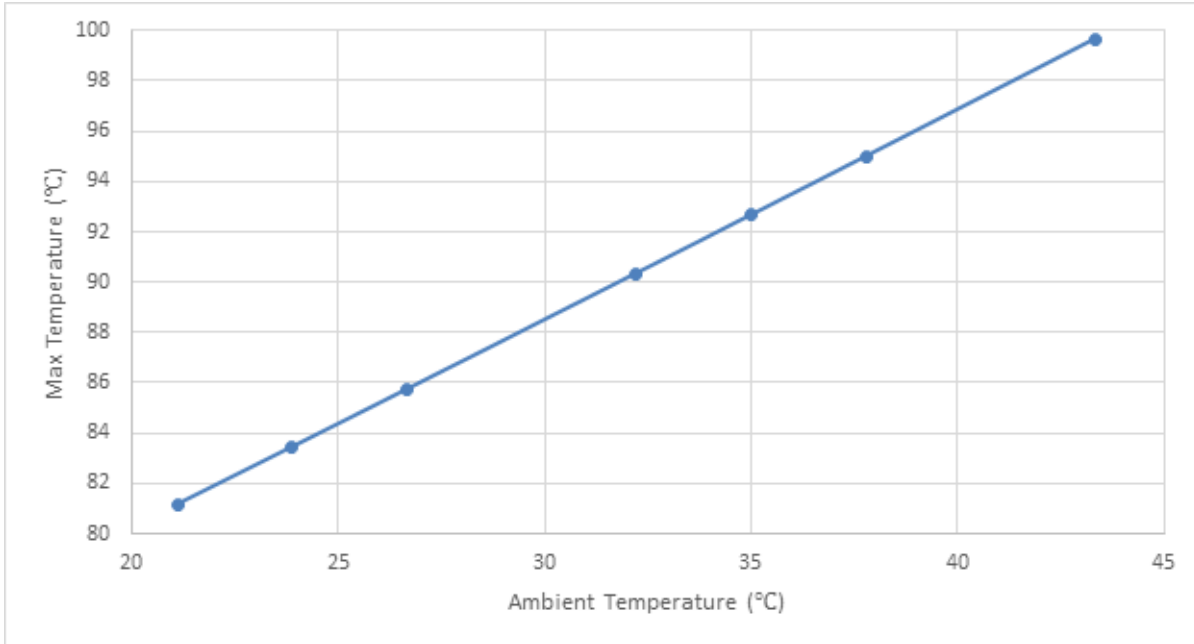


Figure 2-7. Evaluation of ambient air temperature on the computational results

When domain size and boundary conditions are defined as shown in Table 2-2, some of the SDU components are exposed to the SRS ambient conditions, and their thermal responses are dependent on a convective cooling mechanism coupled with daily weather conditions. Figure 2-8 shows the convective cooling mode for a thermal boundary layer established for a wind speed, V_w , on the top external surface of SDU 2A modeling domain (as used for the thermal calculation). The convective cooling rate per unit area, $q_{wall,conv}$, is proportional to the temperature difference between the facility wall and ambient temperatures as shown in Equation (9). The proportional constant is referred to as the heat transfer coefficient, h_w , in the literature. [7]

$$q_{wall,conv} = h_w (T_{wall} - T_{amb}) \quad (9)$$

The coefficient, h_w , was empirically correlated by using a range of different ambient conditions in the literature [7].

$$h_w = 5.678 \left[1.09 + 0.23 \left(\frac{V_w}{0.3048} \right) \right] \quad (10)$$

Where wind speed, V_w , is in m/sec.

Another empirical correlation for wind speed up to 15 meters per second (m/s), equivalent to 34 miles per hour (mph), on a rough horizontal surface [8] is presented:

$$h_w = 3.8V_w + 7.4 \quad (11)$$

where wind speed V_w is in m/sec.

Figure 2-9 compares two empirical correlations for different wind speeds. As shown in the figure, the heat transfer coefficient, h_w , increases linearly with wind speed when wind speed is less than 15 m/sec (as normally experienced at SRS). Sensitivity calculations were performed to assess the effect of changing

wind speed 1 to 6 mph; the thermal results for the two cases are shown in Figure 2-10. The results show that the grout temperatures are not sensitive to the wind speed. For the present analysis, a wind speed of 1 mph was assumed and the heat transfer coefficient at the external wall surface of the SDU was conservatively estimated as $9 \text{ W/m}^2\text{-K}$ (as indicated in Figure 2-9).

As shown in Table 2-2, the optimal domain size and boundary conditions for the SDU thermal model were determined from literature information and the sensitivity analysis.

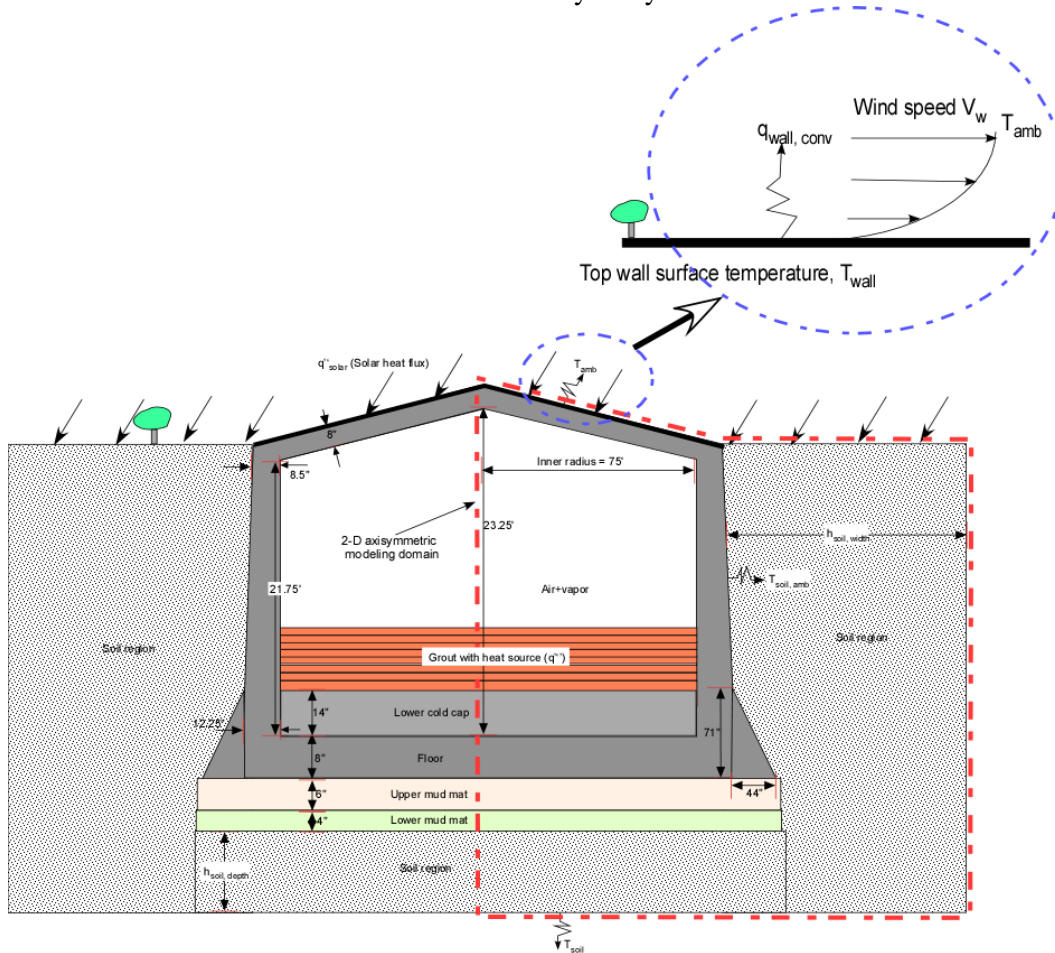


Figure 2-8. Convective cooling mode for a thermal boundary layer established by wind speed V_w on the top external surface of SDU 2A modeling domain as used for the thermal calculations.

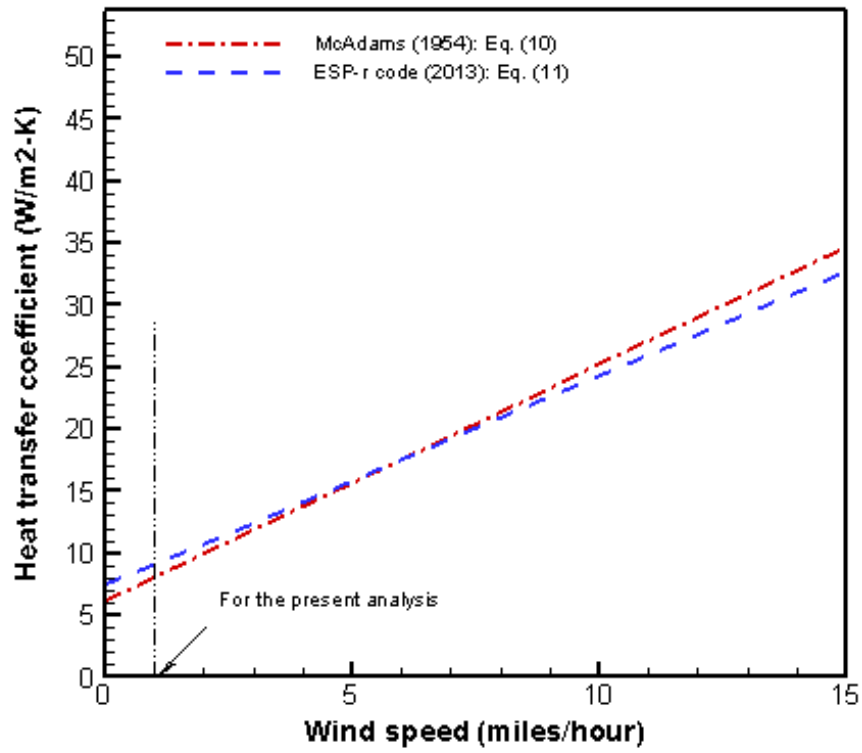


Figure 2-9. Heat transfer coefficients as function of ambient wind speed.

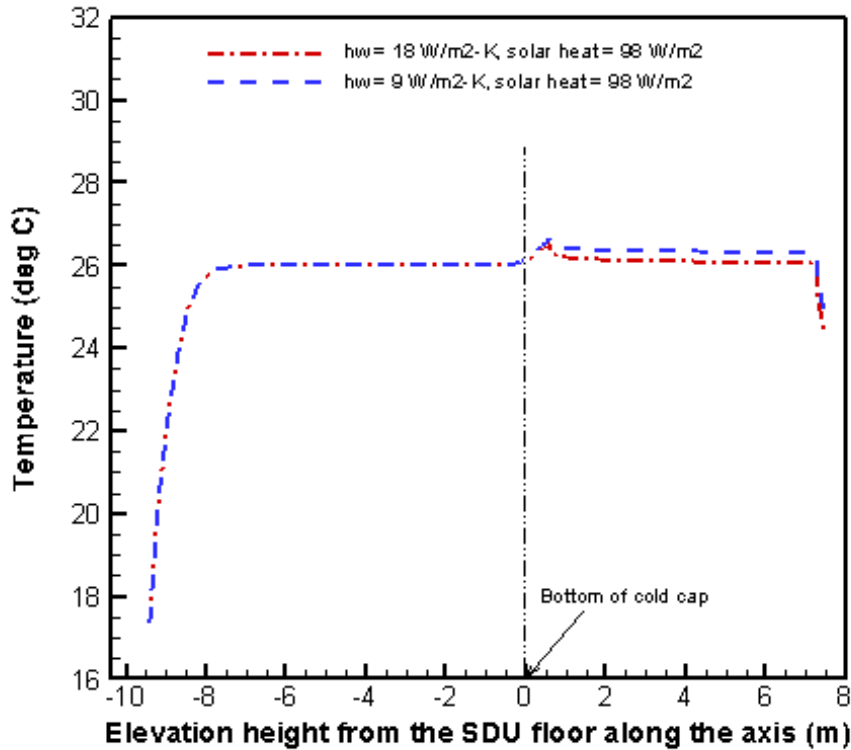


Figure 2-10. Temperature distributions along the vertical centerline

Table 2-2. Domain size and boundary conditions for SDU thermal model

Parameters (Defined in Figure 2-1)	Values
Axi-symmetric boundary	Axially symmetry and no dependency on azimuthal direction ($\left. \frac{\partial T}{\partial r} \right _{r=0} = 0$ and $\left(\frac{\partial T}{\partial \theta} \right) = 0$)
$h_{\text{soil,depth}}$ [14]	30 ft
$h_{\text{soil,width}}$	90 ft
T_{soil} at $h_{\text{soil,depth}} = 30$ ft [14]	17.4°C
Heat flux q'' at $h_{\text{soil,width}} = 90$ ft	No heat flow ($q'' = 0$)
Wall heat transfer coefficient h_w	9 W/m ² -K

2.3 Hydration Heat Source of Grout Material

Low activity salt solution at SRS is stabilized via mixing with blast furnace slag, fly ash, and ordinary Portland cement to form a cementitious grout. This grout is then pumped into an SDU in a series of layers where it cures into a low permeability saltstone. During the curing process of the cementitious grout, two types of thermal heat are produced. They are radionuclide decay heat and hydration heat, both of which raise the temperature of the grout emplaced in the SDU. The hydration heat is generated by an exothermic chemical reaction during the grout curing process, and it is highly dependent on chemical compositions of grout material and aging time.

The decay heat is mainly due to the radioactive decay of Cs-137 radionuclide contained in saltstone. The decay heat is estimated to be about 1.9653×10^{-4} W/kg as provided by the reference [19]. Dividing the decay power (1.9635×10^{-4} W/kg) by the specific heat capacity of grout (1,940 J/kg-K) shows that the temperature of the grout would rise approximately 3°C in a year, assuming no heat loss. For comparison purposes, during a grout pouring day (12/14/2012), the max temperature inside SDU 2A rose approximately 15°C during active pouring. SDU 2A was idle the following day (i.e. there was no grout pouring on 12/15/2012) and the max temperature inside the SDU was found to drop approximately 5°C between the 14th and 15th. Hence, the temperature rise experienced in the SDU grout during an one-day pour was considerably higher than the temperature rise expected from rad decay in one year. Furthermore, the temperature drop experienced between the day of the grout pour and the subsequent idle day was greater than the temperature rise that can be generated by rad decay in one year. Therefore, the radioactive decay heat is not considered for the analysis because it is negligibly small compared to the hydration heat. The heat generated by the grout hydration is dissipated into the surrounding SDU concrete wall, and eventually, the grout cools into thermal equilibrium with the underground soil and ambient weather conditions in contact with the SDU boundary.

As shown in Figure 2-11, the grout heat generation is dependent on grout formulation, resulting in different rate of hydration heat generation. For the present thermal calculations, two different sources of the hydration heat were modeled: a 45:45:10 saltstone mixture for SDU 2A (i.e., the saltstone is made using a dry feed consisting of 45% blast furnace slag, 45% fly ash, and 10% ordinary Portland cement) and a 60:40 cement-free saltstone mixture for SDU 6 (i.e., the saltstone is made using a dry feed consisting of 60% blast furnace slag and 40% fly ash). The heat source for SDU 2A was used for benchmarking of the model against the thermocouple data to verify the modeling results. A volumetric heat source term, q'' , in the energy equation, Equation (4), is required as a model input for the thermal calculations.

The source terms for two different types of grout formulation were polynomially fitted as function of transient time by using the experimental data provided by SRR customer [4]. When the transient time is longer than 1320 hours, it was exponentially fitted as shown in Appendix A. Based on the source curves of Figure 2-11, the heat sources contained in the grout were compared during one-month period of SDU storage. It is noted that the heat sources are rapidly reduced by a factor of 120 during the one-month period. When a volumetric heat source, q'' , is in watts per m³ (W/m³), storage time, t, should be in hours (h). Transient source terms for the SDU 2A benchmarking task and SDU 6 performance calculations are provided in Appendix A-1 and A-2, respectively.

The curve for the volumetric heat generation rate was used for the solidified grout region as heat source input to the transient temperature calculations over the SDU computational domain. The curve-fitted equations as presented in Appendix A show transient volumetric heat source as function of grout storage time. These heat source curves were used for the present SDU thermal calculations.

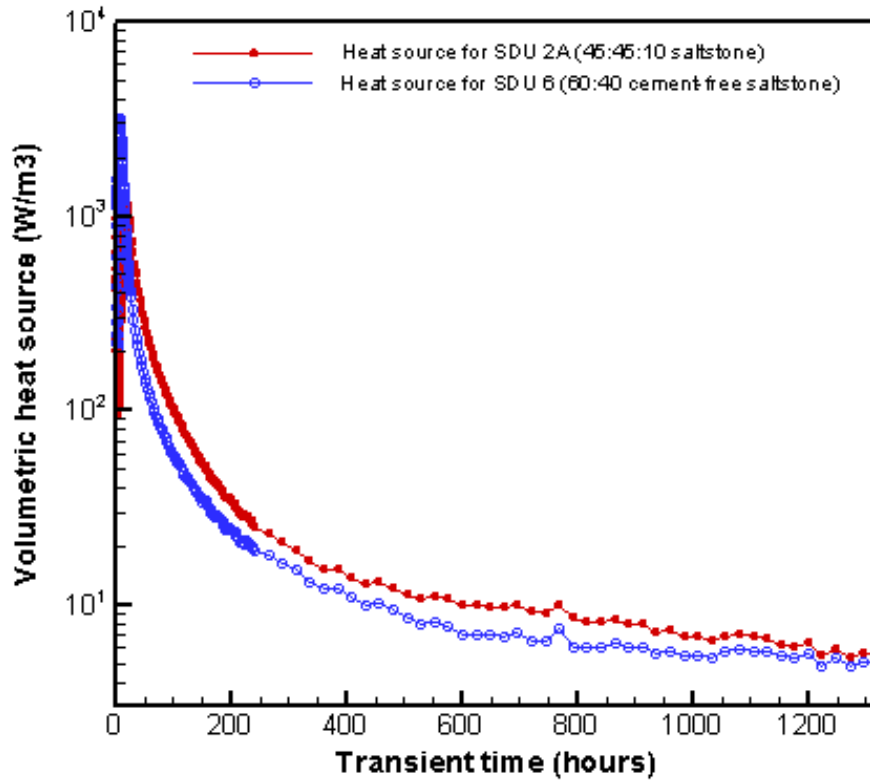


Figure 2-11. Comparison of hydration heat sources between the two different SDU grout formulations

2.4 Ambient temperature and solar heat around the SDU

The hydration heat source defined in Section 2.3 is dissipated by the underground soil media and ambient air in contact with the SDU external boundary. When the high and low ambient temperatures, T_{high} and T_{low} , are provided by the SRNL weather database on a daily basis, the transient ambient temperature, T_{amb} , can be fitted as function of time t (in hour) by the following sinusoidal function.

$$T_{amb} = A - B \cos\left(\frac{\pi t}{12}\right) \tag{12}$$

Coefficients A and B in Equation (12) are given as $0.5(T_{high} + T_{low})$ and $0.5|T_{high} - T_{low}|$, respectively. The coefficients were determined by the SRNL weather data measured on a daily basis.

Figure 2-12 shows ambient temperatures for SDU 2A for a period from August 9, 2012, to June 30, 2014. The temperature curve shown in the figure was used in the transient energy balance equation of Equation (4) as one of boundary conditions for the two-dimensional SDU modeling domain as defined in Figure 2-8.

For the SDU 6 analysis, two coefficients (i.e., A and B) of Equation (12) for transient ambient temperatures were determined by using the average temperatures of the SRNL weather data for three years from 2015 to 2017. Figure 2-13 shows the ambient temperatures used for the SDU 6 thermal calculations.

The solar heat of SDU dome is accounted for in the present thermal model. The average solar insolation on the horizontal and side surfaces under the atmospheric conditions of Equation (12) is provided by the literature information [10]. The solar heat shown in Table 2-3 was applied to the external surface of the facility for the day- and night-time hours to estimate maximum grout temperatures in a realistic way, taking into account for the atmospheric effects such as rain and cloud cover.

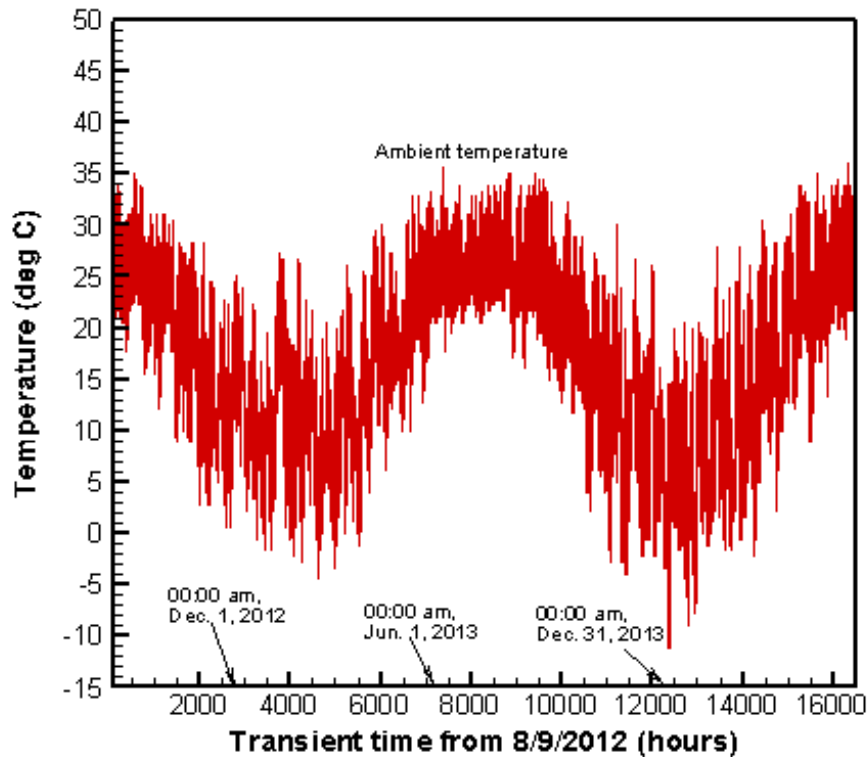


Figure 2-12. Ambient temperatures for SDU 2A between August 9, 2012 and June 30, 2014.

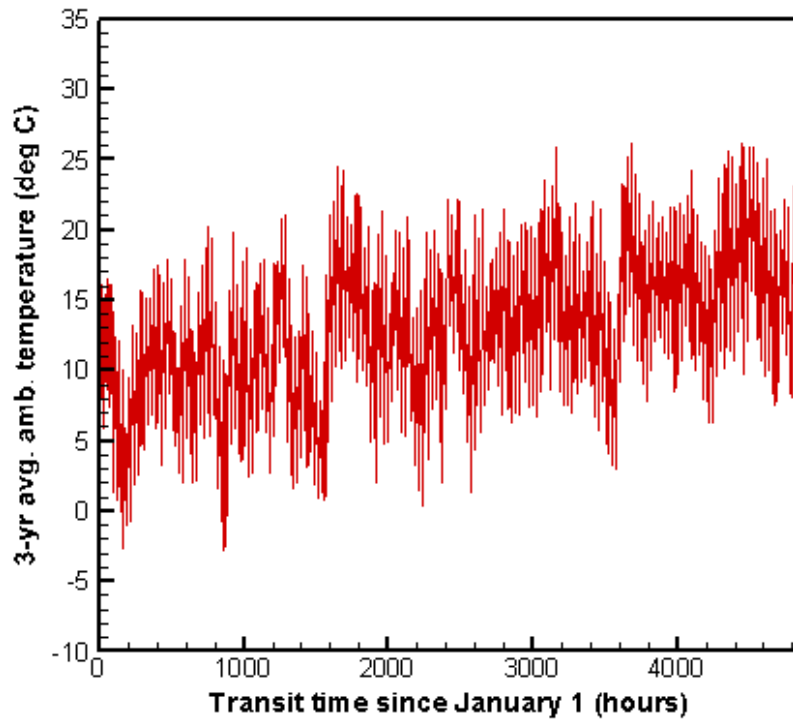
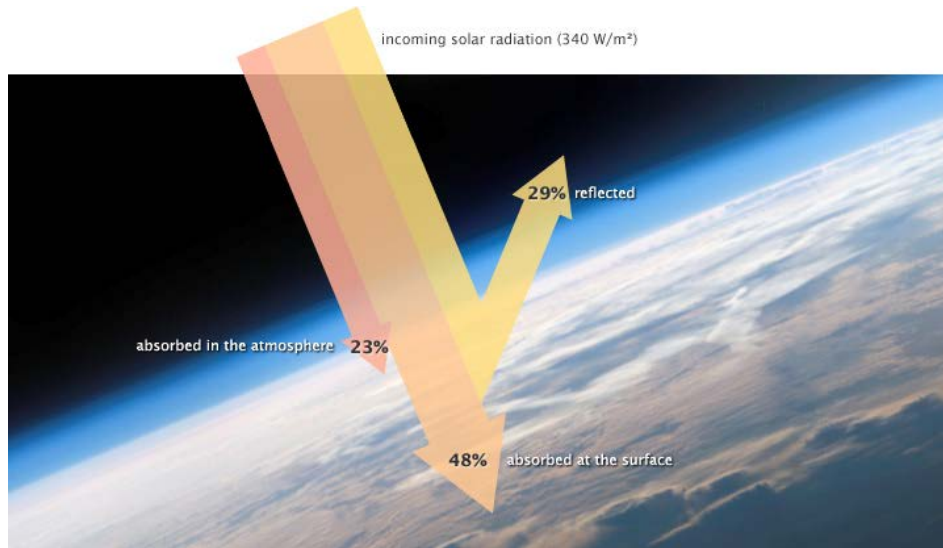


Figure 2-13. Ambient temperatures for SDU 6 during a five-month period of January to July.

Table 2-3. Solar heat for the SDU facility



(As Provided by NASA Earth Observatory [10])

Location	Solar heat flux (W/m ²)	Absorptivity [17]	Solar heat flux absorbed into surface (W/m ²)*
Top surface (Concrete: white paint)	163.2	0.3	48.96
Side surface** (Concrete: white paint)	81.6	0.3	24.48
Top surface (Soil: green/brown)	163.2	0.6	97.92

Note: * Applied to the SDU external surfaces on a 24-hour daily basis

**For the SDU 6 calculations

2.5 Grout Pouring Schedule of SDU facility

Low activity salt solution at SRS is mixed with cementitious grout; the mixed grout is then pumped into the SDU in a series of layers where it cures into a solidified saltstone. During the curing process of cementitious grout, hydration heat is transiently produced. The heat produced by fresh grout serves to raise the temperature of the grout emplaced in the SDU facility; the total time-dependent hydration heat produced by the grout is dependent on the grout pour schedule. In this case, the grout layer filled at each pouring should account for the age of the poured grout using a Lagrangian approach, as shown in Figure 2-14, because the heat generation from the grout is highly dependent on its residence time in the SDU. The grout pouring schedule comprises scheduled times for grout production separated by planned production outages when no grout is added to the SDU; hence, the grout pouring schedule has a major impact on the time-dependent heat generated in the SDU.

The grout pours are implemented in a discrete Lagrangian way as shown in Figure 2-14. For a layer that was poured in real life between times t_0 and $t_0 + \Delta t$:

- The model layer is assumed to be poured instantaneously at time t_0 .

- The model layer is assumed to be of the same age.
- As soon as the grout layer is formed at time t_0 , heat source of the layer is turned on at an averaged grout age of $(\Delta t/2)$.

As mentioned above, a transient thermal assessment of the SDU grout was made for the work in a Lagrangian approach.

Figure 2-15 shows the grout pouring schedule used for the thermal calculations of SDU 2A. Detailed schedules used for the SDU 2A calculations is provided in Table A-3. Based on the modeling boundary conditions established by the benchmarking analysis of SDU 2A, Figure 2-16 shows the grout pouring schedule used for the thermal performance calculations for SDU 6. As shown in the figure, the grout schedule for SDU 6 has a repetitive sequence of 12.3 days of continuous pouring followed by 46.6 days idling, until the SDU is filled. In Appendix A, Table A-3 and Table A-4 show the corresponding grout schedules for SDU 2A and SDU 6 that were used for the modeling calculations. It is noted that Table A-4 shows the saltstone pouring schedule corresponding to approximately half-filled SDU 6.

2.6 Discretization of Modeling Domain

The modeling domain for the SDU was determined using a series of sensitivity analyses and literature information, which is summarized in Table 2-2. The domain includes SDU structure, concrete wall, and soil region as shown in Figure 2-8. The domain geometry was created and meshed using the ANSYS-FLUENT software. The surface of the modeling domain is decomposed into component surfaces that allow greater mesh accuracy and efficiency. In regions that are expected to experience larger temperature gradients, the component surface is assigned by a greater mesh density to increase solution accuracy. The vapor space of the SDU is an example of a component surface with a greater mesh density, as well as regions on and near conducting/convecting/radiating surface boundaries. Conversely, the mesh density is smaller on component surfaces that are expected to experience smaller temperature gradients, such as the thick concrete and soil portions of the domain. This approach to modeling/meshing the SDU decreases the time of computation and increases the solution accuracy. The resulting number of computational mesh nodes over the modeling domain was approximately 30,000 nodes for SDU 2A. Figure 2-17 illustrates the computational meshes over the modeling domain containing the geometry of SDU 2A for the benchmarking test against the thermocouple data. The number of discretized meshes for SDU 6 was established as approximately 110,000 for the thermal performance calculations, as shown in Figure 2-18.

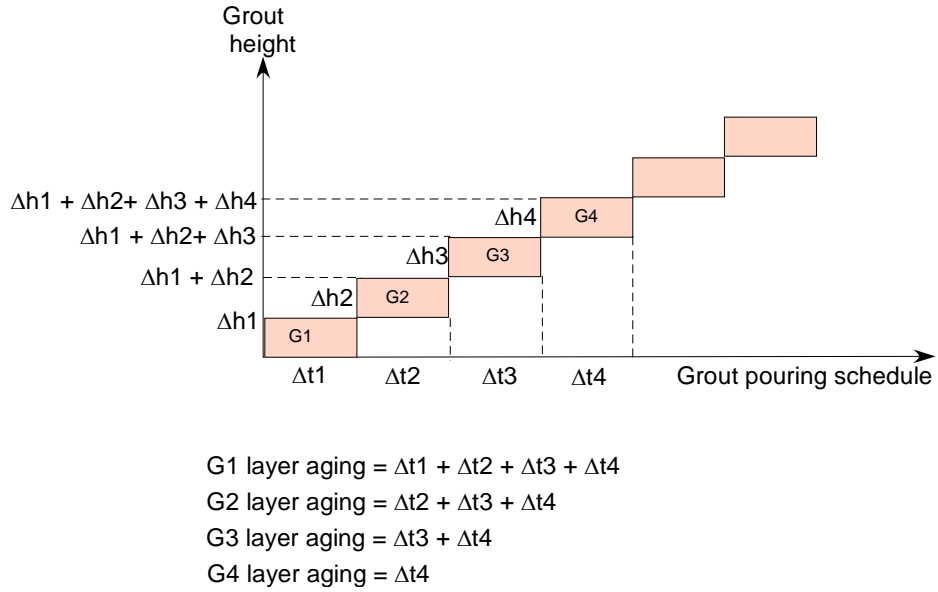


Figure 2-14. Transient grout height above the SDU 2A floor during the grout pouring period.

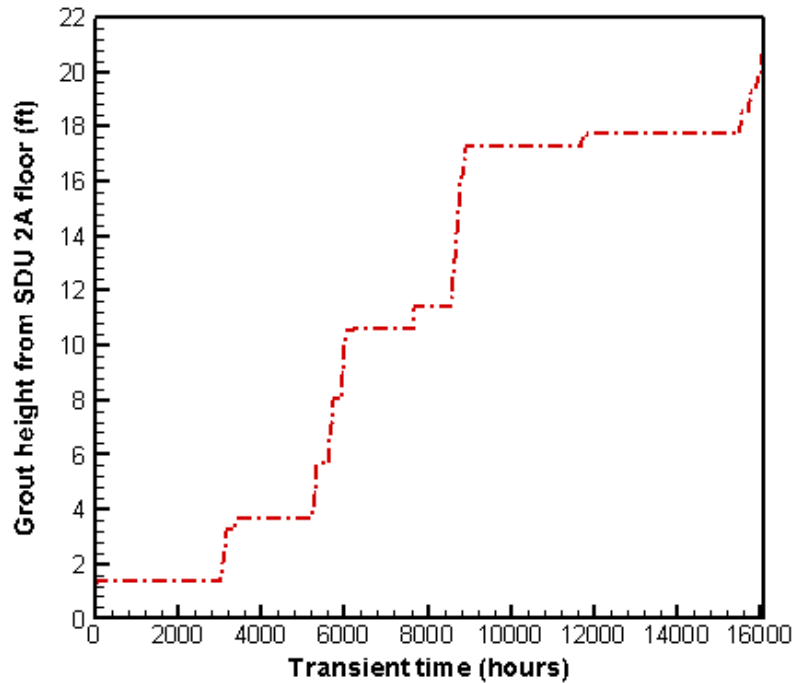


Figure 2-15. Transient grout height above the SDU 2A floor during the active filling period of August 10, 2012 to June 11, 2014.

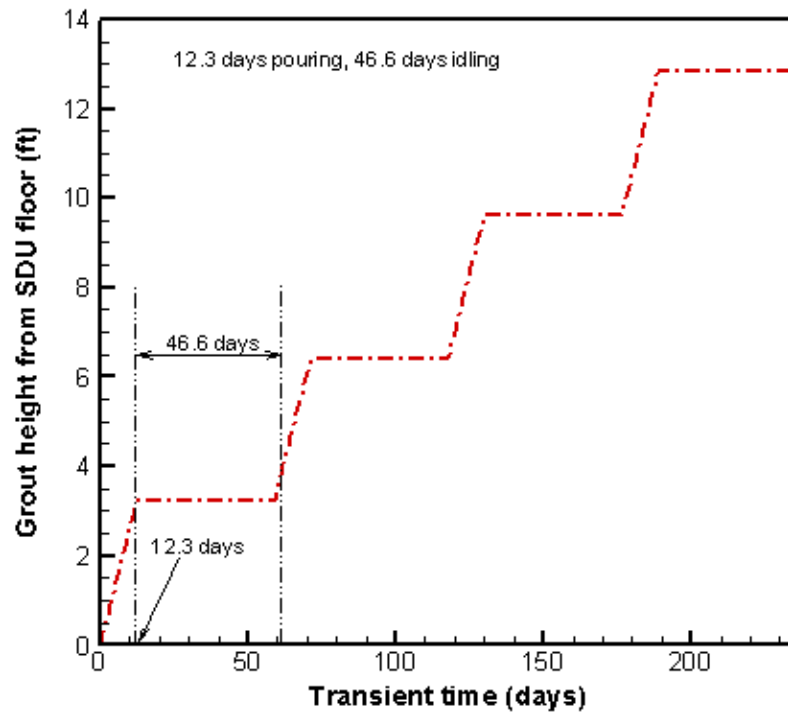
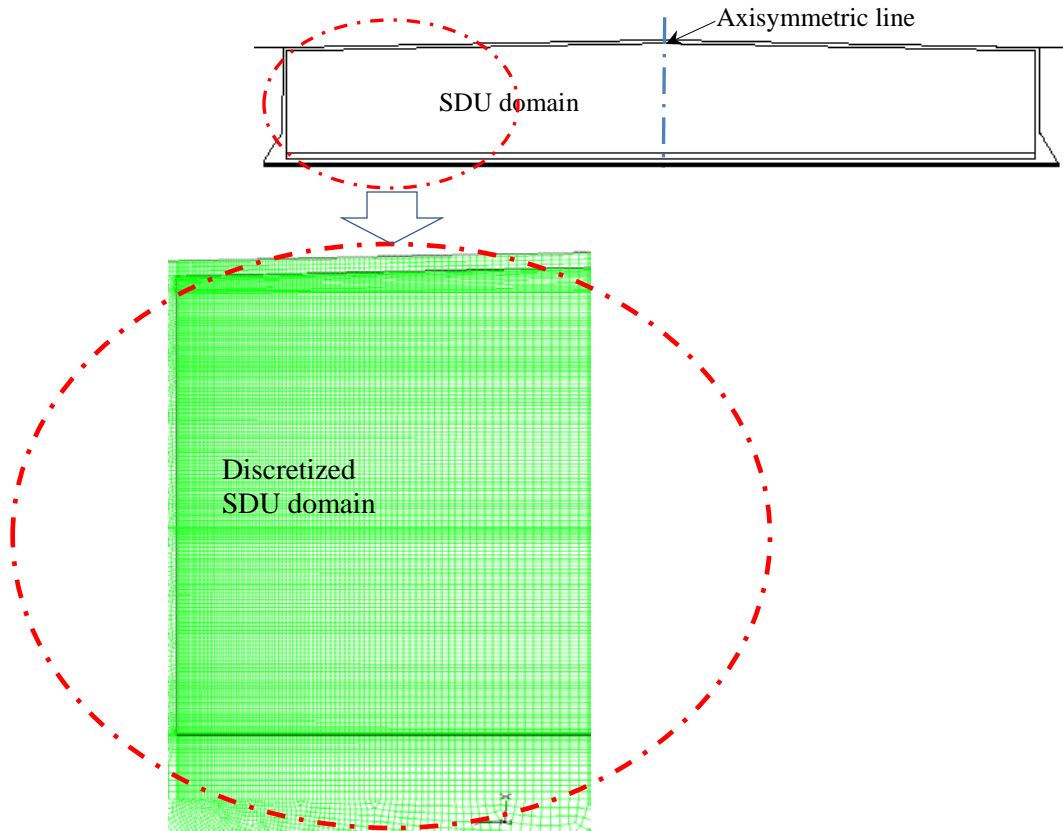
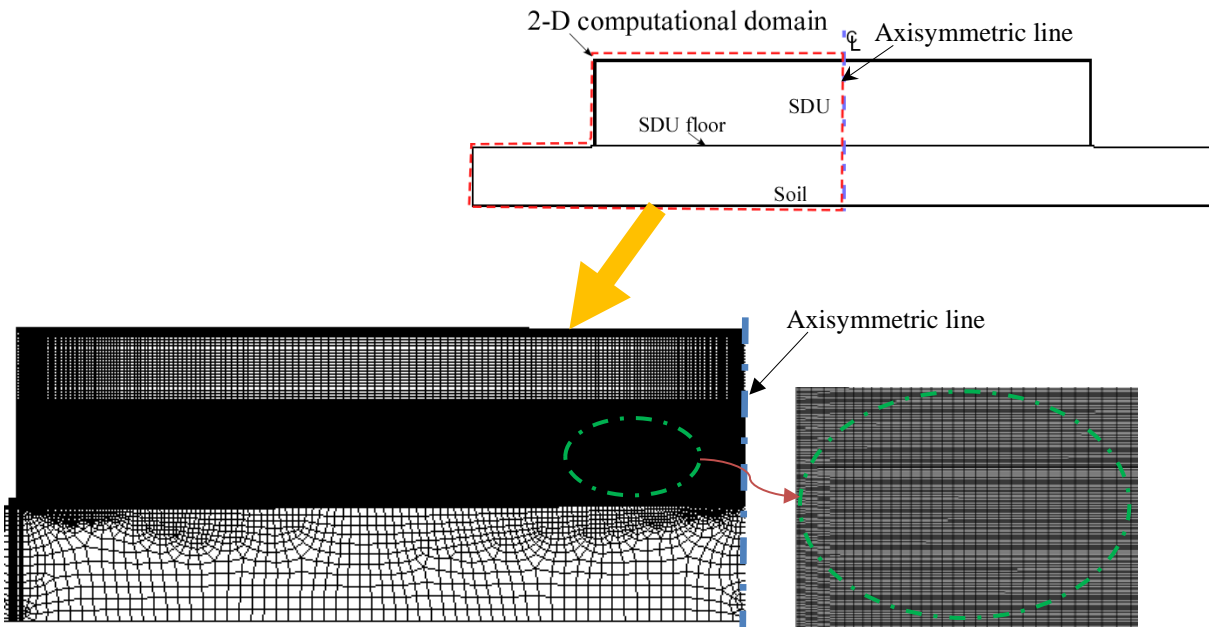


Figure 2-16. Transient grout heights above the SDU 6 floor during the grout pouring period.



(~30,000 computational meshes based on axi-symmetric modeling domain)

Figure 2-17. Two-dimensional computational meshed for SDU 2A modeling domain as used for the thermal benchmarking calculations.



(~110,000 meshes for the 2-D axisymmetric computational domain boundary)

Figure 2-18. Two-dimensional computational meshes for the axisymmetric modeling domain of SDU 6 as used for the thermal performance calculations.

3.0 Benchmarking Test for SDU 2A

As shown in Figure 2-2, a transient simulation model was developed by taking an axisymmetric and two-dimensional CFD approach in order to predict the temperatures attained in SDUs during the saltstone grout addition, and its subsequent storage period. The grout material contains a transient hydrating heat source as shown in Figure 2-11. The model should be capable of predicting the transient temperatures at point locations within the poured grout, the air space overlying the poured grout, and the interior/exterior surfaces of the SDU structure. For the modeling calculations, the grout pouring schedule is a key input parameter. For this case, other input parameters, such as thermal and material properties of the SDU components, heat source term, boundary conditions and domain discretization, were completely set up for the modeling domain (as established in earlier sections). The CFD model for SDU 2A was benchmarked against the thermocouple measurements to ensure that the model-predicted transient grout temperatures were conservative. The SDU 2A modeling domain is defined in Figure 2-8. Thermocouples in SDU 2A are present every foot starting at 0.5 ft above the SDU floor. It is noted that although there are three thermocouple trains at each elevation, local temperatures at both of Train A and Train B are not able to be differentiated under the axisymmetric approach because of the same radial distance from the center of the SDU 2A. The location of thermocouples at three different elevations of the SDU 2A domain is depicted in Figure 3-1.

When the daily ambient temperatures (Figure 2-12) and the transient heat source (Figure 2-11) are applied to the computational modeling domain of SDU 2A with the boundary condition of 24-hour insolation, the modeling calculations were performed using the solution method described in Section 2.1. Other boundary conditions used at the boundary of the modeling domain are presented in Table 2-2. The calculation results show that when SDU 2A is uniformly filled with the hydrating grout material (up to a height of approximately 3.5 ft. above the SDU floor), the model consistently overpredicts the maximum grout temperature by about 10°C in comparison to the measured data, as shown in Figure 3-2. Figure 3-3 compares the modeling predictions and test data at the thermocouple position 2.5 ft Train A/B in the grout region of SDU 2A. The grout temperatures for Train C at a position of 10.5 ft are compared between the modeling predictions and the thermocouple data in Figure 3-4. As shown in the figures, the modeling predictions are always higher than the test data. Figure 3-5 shows the modeling predictions of maximum grout temperatures in comparison with the thermocouple data for the grout region of the SDU during the entire filling period (combined with intermittent idling) of about 16,000 hours. From the benchmarking results, it is noted that when the grout level exceeds approximately 17 ft., the model underpredicts the grout temperatures by about 4°C during the non-production idling periods; this is possibly due to the uneven accumulation of grout inside the SDU. When a grout layer is radially flat with the same thickness under uniformly distributed heat source, the grout temperature at a given elevation theoretically decreases toward the wall of the SDU because of heat loss at the domain wall boundary. As shown in Figure 3-6, when the grout level is higher than 12ft above the SDU floor, the grout temperature measured at the thermocouple position of 10.5ft is increased by about 10°C with the radial distance increased from 10 ft (Train A/B) to 50 ft (Train C). This suggests that the grout may have an uneven thickness or nonuniform composition.

Comparing the predicted grout temperatures with the actual SDU 2A thermocouple data, it can be concluded that when the grout formulated for SDU 2A is poured into the facility (per the pouring schedule of Figure 2-15), the model predicts the grout temperatures in a conservative manner, and its maximum temperature remains below 80°C.

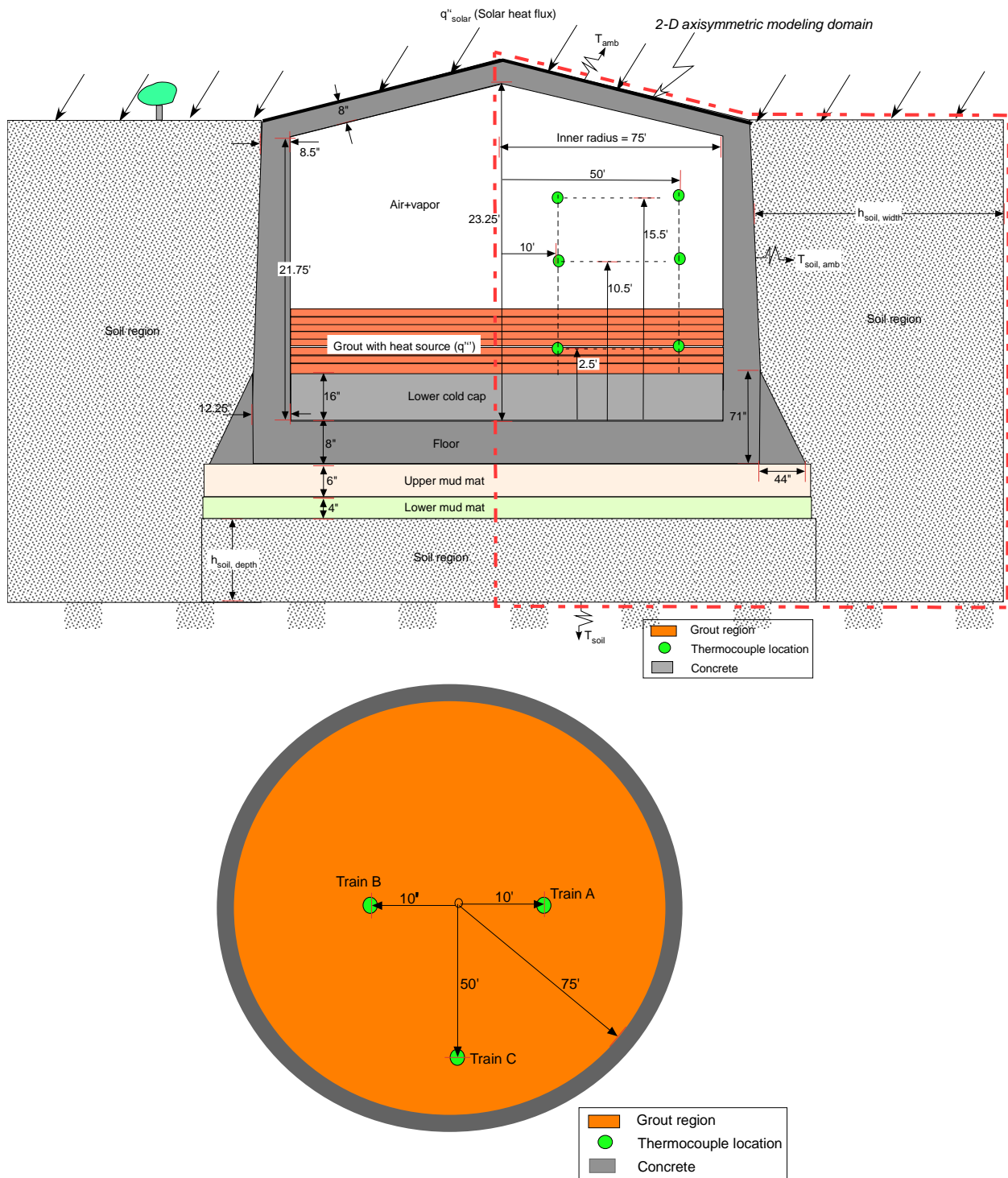


Figure 3-1. Thermocouple locations for the SDU 2A facility.

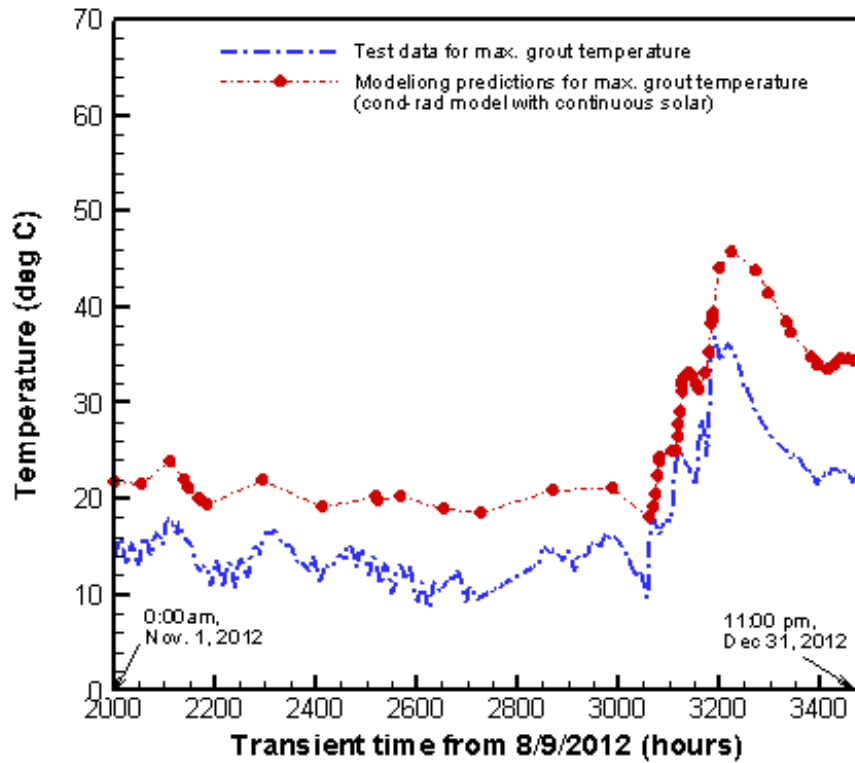


Figure 3-2. Comparison of the modeling predictions and SDU 2A thermocouple data for the grout height less than 3.5 ft.

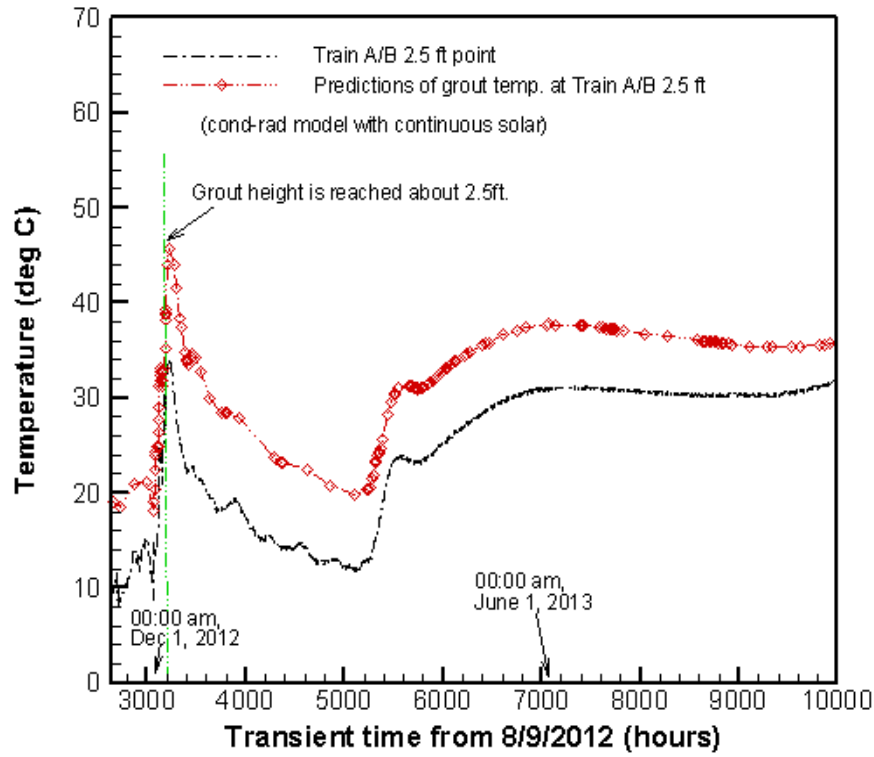


Figure 3-3. Comparison of the modeling predictions and SDU 2A thermocouple data at the thermocouple position 2.5 ft for Train A/B

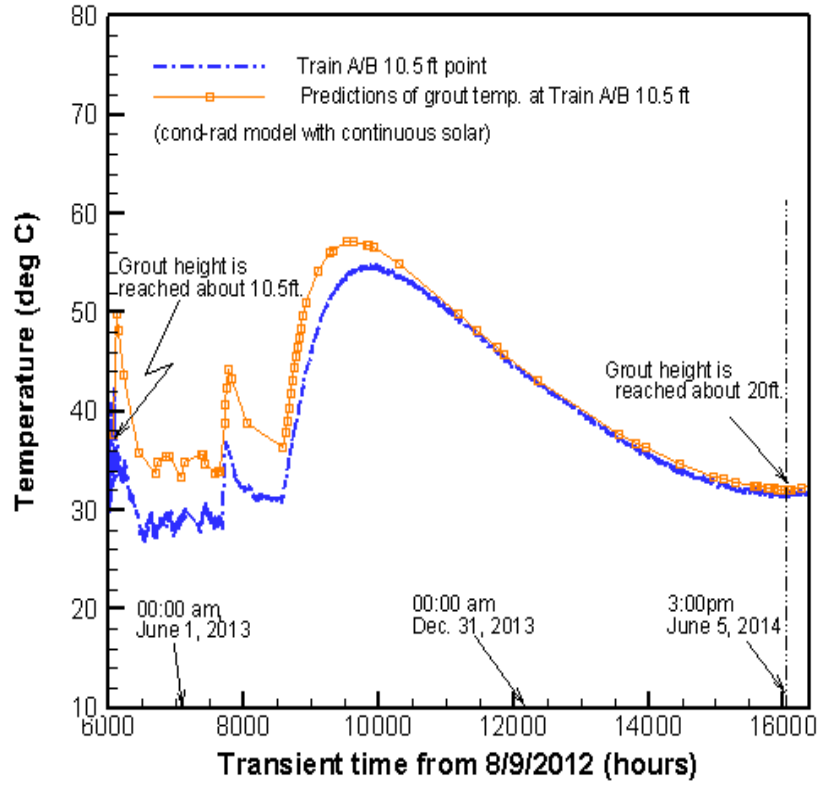


Figure 3-4. Comparison of the modeling predictions and SDU 2A thermocouple data at the thermocouple position 10.5 ft for Train A/B

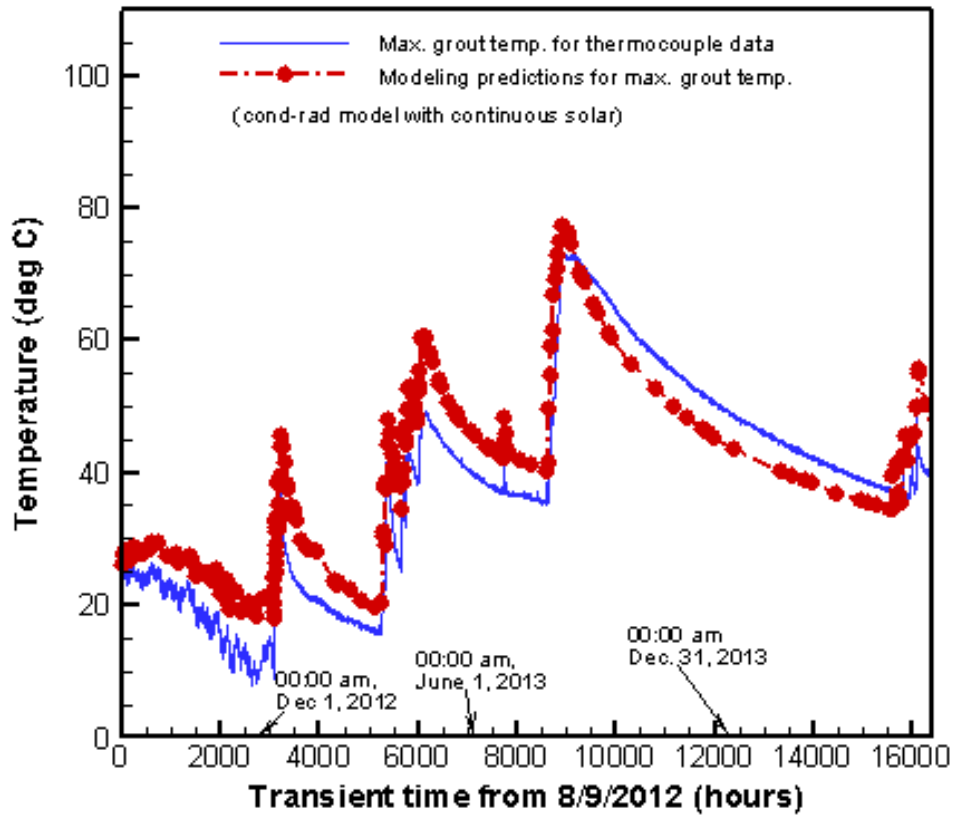


Figure 3-5. Comparison of maximum grout temperatures between the modeling predictions and SDU 2A thermocouple data at the completion of pouring

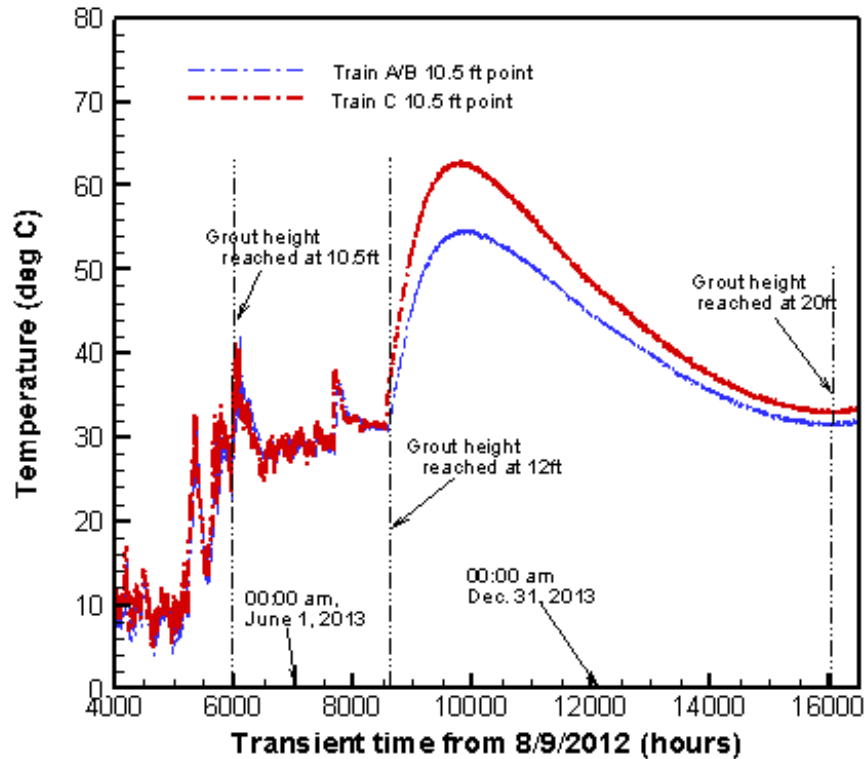


Figure 3-6. Comparison of transient SDU 2A thermocouple data at position 10.5 ft.

4.0 Results and Discussion

A CFD simulation model was developed to predict the transient temperatures attained in SDUs during and after the addition of a hydrating grout material containing a heat generation source. The basic scope of work for the present work is illustrated in Figure 2-2. As shown in the figure, a transient two-dimensional CFD approach was conducted using an axisymmetric geometry of the SDU. The hydration process of the grout material produces thermal heat from an exothermic chemical reaction. In this work, several different types of scoping analysis were performed to define the optimal modeling domain boundary. This included parametric sensitivity calculations of soil thickness, soil conductivity, and ambient boundary conditions. For the benchmarking calculations, the top surface of the grout layer was assumed to be horizontally flat when the SDU was filled with grout material.

The present work has considered two different disposal units, namely, SDU 2A and SDU 6. Prior to performing the thermal calculations for SDU 6, the benchmarking test for the SDU 2A was performed to establish the validity of the solution method, and to compare the computational modeling predictions with the thermocouple test results. Based on the solution method and the boundary conditions, as established by the benchmarking test, the CFD calculations were performed to predict the transient temperatures at point locations within the poured grout, the overlying vapor space, and the interior and exterior surfaces of the SDU structure. The model developed in this study can be used to predict grout temperatures within an SDU for different saltstone pour schedules, SDU designs, and saltstone compositions (with varied thermal properties).

For the thermal calculations of the SDU 6 domain as defined in Figure 1-2, the conduction cooling mechanism coupled with radiation were considered for a conservative estimate of the saltstone temperatures and for computational efficiency. In this case, transient thermal heat produced by the hydration reactions of the saltstone grout is dissipated through ambient air and ground soil media. The model simulates a nominal grout flowrate of 150 gpm with 12.3 days of pouring and 46.6 days idle (i.e., without pouring). On a daily basis, 216,000 gallons of grout are poured into the SDU 6 vault. This corresponds to a grout height of approximately 0.27 ft. The pouring operation is completed when the top surface of the poured grout reaches a height of 41 ft above the SDU floor. Ambient temperatures were based on the hourly temperatures measured by SRNL [18]. For the boundary conditions, a transient sinusoidal equation was used by fitting the temperatures averaged over the three-year period of January 2015 to January 2017, as shown in Figure 2-13. Detailed thermal properties of the SDU components and modeling boundary conditions of the domain for the calculations are summarized in Table 2-1 and Table 2-2, respectively. The grout pour schedule for the SDU 6 model is shown in Figure 2-16. Appendix A-4 shows each predetermined layer's start time and end time.

The grout pouring schedule comprises a series of pouring and idling lift schedules. For the thermal analysis of the SDU 6, each lift has grout production of 12.3 days followed by planned production outages of 46.6 days with no grout addition to the SDU. In this case, the grout pouring schedule has a major thermal impact on the time-dependent heat generation imbedded in a grout layer of the SDU. The time-dependent additions of the grout layer were implemented in a discrete Lagrangian way as shown in Figure 2-14. Specifically, for a discretized layer that was poured in real life between times t_0 and $t_0 + \Delta t$, the pouring time Δt was set up to be 12 hours (equivalent to a layer thickness Δh of 0.1307ft) when a grout nominal flow of 150 gpm is continuously poured into the SDU 6 vault.

As shown in Figure 4-1, the SDU 6 model runs are stopped at two lifts of the pouring and idling operation. The modeling results show that when grout pouring started on January 1, the maximum grout temperatures attained are 52°C at the end of the 1st lift pouring on January 13 and 56°C at the end of the 2nd lift pouring on March 13. It is noted that the 2nd peak grout temperature is about 4°C higher than the 1st peak because of the increased ambient temperature. These are consistent with the sensitivity results that ambient temperature has a linear effect on the maximum grout temperature of the SDU as discussed earlier. This model simulation used a pour schedule 12.3 days (295 hours) pouring followed by long idling times (1118 hours). This idling time after the pour allows the grout heat to be dissipated into the ambient air and the adjacent soil media prior to the next pour. Figure 4-2 compares transient temperature profiles along the vertical centerline of SDU 6 for different pouring times during the pouring period of 295 hours. The results show that for each of the transient times there is a large temperature gradient at the interface of the grout and its surrounding media such as the concrete wall or SDU air region, resulting in a rapid heat dissipation of the saltstone grout containing the hydration heat, as defined in Appendix A-2.

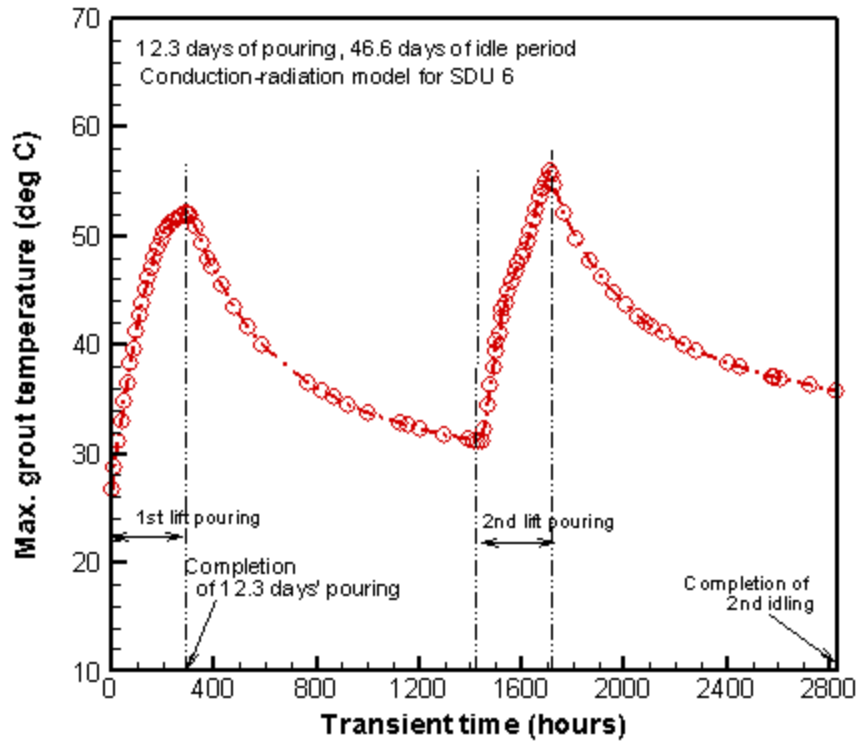


Figure 4-1. Modeling predictions for the SDU 6 facility for the operation schedule of 12.3 days pouring and 46.6 days' idle

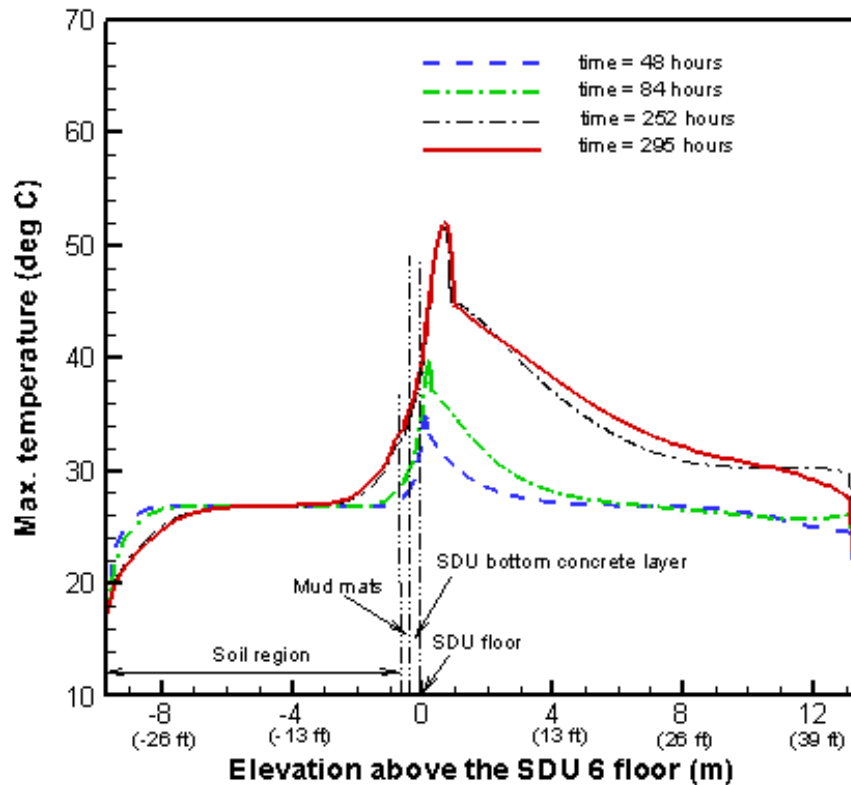


Figure 4-2. Transient temperature profiles along the vertical centerline of the SDU 6 facility

5.0 Conclusions

A CFD model was developed to predict the transient temperatures attained in SDUs when permanently filled with a hydrating grout material containing a transient heat source. A transient two-dimensional CFD approach was used by assuming the SDU is symmetrical along the axial direction. The CFD model was developed with the commercial software, ANSYS-FLUENT™. Although the modeling domain was initially constructed by three heat transfer modes of conduction, convection, and radiation, the main calculations of the SDU model were performed by using a conduction-radiation cooling mechanism without convection; this provided a conservative estimate of the saltstone temperatures and also enhanced computational efficiency.

The thermal model has been developed for two SDUs at SRS; namely, SDU 2A and SDU 6. SDU 2A is cylindrical unit measuring 150 ft.in diameter and 22 ft. in height, and has a grout capacity of approximately three million gallons. SDU 6 is a larger scale unit measuring 375 ft. in diameter and 43 ft. in height, and it has a grout capacity of over thirty million gallons. Prior to performing the thermal calculations for SDU 6, a benchmarking test for the smaller unit (SDU 2A) was performed to establish the solution method, and to verify the computational results with actual grout temperature data measured within the unit. Based on the Lagrangian discrete method and boundary conditions established by the benchmarking test, the CFD calculations were performed to predict the transient temperatures at point locations of the poured grout and the overlying vapor space within the SDU 6 structure.

From the benchmarking results, it is noted that when the grout level becomes higher than about 17 ft., the model underpredicts the grout temperatures by about 4°C during idling times of when no grout is added to the SDU. This under prediction is possibly the result of uneven grout accumulations or non-uniform grout formulations. The results show that when the grout formulated for SDU 2A is poured into the facility, the model consistently predicts the grout temperatures in a conservative manner, and its maximum temperature remains below 80°C. In addition, it was confirmed that all boundary conditions applied to the model maintained the conservative nature of the predicted temperature data.

Based on the discrete Lagrangian method and boundary conditions established by the benchmarking work, the SDU 6 model was developed for a quantitative assessment of the transient temperatures at local positions of the poured grout within the SDU. A pour schedule of 12.3 days of grout filling followed by 46.6 days of non-production (idling) time was used for the dynamic computer simulation of the saltstone pouring into SDU 6. The modeling results show that when grout pouring started on January 1, a maximum grout temperature of about 52°C is reached (at the end of pouring on January 13). In this case, it is noted that the ambient temperature has a linear effect on the maximum temperature of the SDU grout as discussed in the sensitivity analysis. Therefore, when ambient temperature during the summer time is about 20°C higher than that of the winter time on the average, the results indicate that the maximum grout temperature for the SDU 6 unit is expected to be well below 95°C. The model developed in this study can be used to predict grout temperatures within an SDU for different saltstone pour schedules, SDU designs, and saltstone compositions (with varied thermal properties).

6.0 References

1. “Saltstone Facility: Documented Safety Analysis”, WSRC-SA-2003-00001, Rev. 14, December 2017.
2. S. Simner, Technical Task Request: “*Development of Computer Simulation to Predict Temperatures in Saltstone Disposal Units (SDUs)*”, G-TTR-Z-00013, Rev. 0, April 18, 2018.
3. Task Technical and Quality Assurance Plan for Thermal Analysis of Saltstone Disposal Units, SRNL-RP-2018-00616, July 2018.
4. J. E. Mangold, “Recommended Input Values for Thermal Model Development”, SRR-CWDA-2018-00074, Revision 0, October 18, 2018.
5. J. Dewberry, “Transient Thermal Analysis of SDU6 Concrete Tank with Grout”, CACL-ME-5539-0001, Rev. 0, December 5, 2016.
6. C-CC-Z-00042, *Z-Area Saltstone Disposal Site SDU6 Tank Design Concrete Wall Column Section Details*, Savannah River Site, Aiken, SC, Rev. 0, November 7, 2012.
7. W. H. McAdams, *Heat Transmission*, 3rd Edition, McGraw-Hill Book Company, Inc. New York, 1954.
8. M. Mirsadeghi, D. Cóstola, B. Blocken, J.L.M. Hensen, “Review of external convective heat transfer coefficient models in building energy simulation programs: implementation and uncertainty”, *Applied Thermal Engineering*, March 2013.
9. I. N. Hamdhan and B. G. Clarke, “Determination of Thermal Conductivity of Coarse and Fine Sand Soils”, *Proceedings of 2010 World Geothermal Congress*, Bali, Indonesia, April 25 – 29, 2010.
10. NASA’s Featured Article, “Earth’s Energy Budget”, Earth Observatory, NASA, <https://earthobservatory.nasa.gov/Features/EnergyBalance/page4.php>
11. H. N. Guerrero, S. Y. Lee, D. A. Eghbali, and T. J. Steeper, "Heat Transfer Aspects of Interim Dry Storage of Aluminum-Clad Spent Nuclear Fuel", *1996 ANS Embedded Topical Meeting on DOE Spent Fuel and Fissile Materials Management*, Reno, Nevada, June 10-16, 1996.
12. S. T. Thynell, “Discrete-ordinates method in radiative heat transfer”, *International Journal of Engineering Science*, Volume 36, Issues 12-14, September –November 1998, pp. 1651-1675.
13. S. Y. Lee, "CFD Modeling of Natural Convection within Dry Spent Nuclear Fuel Storage Canister", *ANS Proceedings of the 1996 National Heat Transfer Conference*, HTC-vol. 9, pp. 213-224, August 1996.
14. SRS Environmental Restoration Data Management System (ERDMS) website: <http://www.srs.gov/deidms/index.html>
15. S. E. Aleman, G. P. Flach, L. L. Hamm, S. Y. Lee, and F. G. Smith, III, 1993, “FLOWTRAN-TF Code Software Design (U)”, WSRC-TR-92-532, Savannah River National Laboratory, Westinghouse Savannah River Company, February 1993
16. S. Y. Lee and D. W. Vinson, “Thermal Evaluations for L-Basin Drain-Down SNF Storage Facility”, SRNL-STI-2016-00587, Savannah River National Laboratory, December 2016.
17. The Engineering ToolBox website: Absorbed solar radiation by surface color, <http://www.EngineeringToolBox.com>.
18. SRNL home page: https://weather.srs.gov/weather/climate_data
19. ATKINS report, “SDU2A Transient Thermal Sensitivity Analysis”, RPT-5539-ME-0024, Contract Number: SRRA084094, May 25, 2017.
20. J. Seaman, “Thermal Properties of Saltstone Simulants”, SRRA099188-000004 Rev. B, October 17, 2018.

Appendix A. Transient Thermal Source and Grout Pour Schedule

A-1. Transient heat source terms for SDU2A grout region

For time t (hours) of $0 < t < 0.24$ hours,

$$q''' = A + Bt + C t^2 + Dt^3 + Et^4 + Ft^5 + Gt^6 + Ht^7 + It^8 + Jt^9$$

where

$$A = 0.0$$

$$B = 2.07273154883735750000 \times 10^5$$

$$C = -4.73727966385484950000 \times 10^6$$

$$D = 2.01537892317851670000 \times 10^7$$

$$E = 6.82899388191934590000 \times 10^8$$

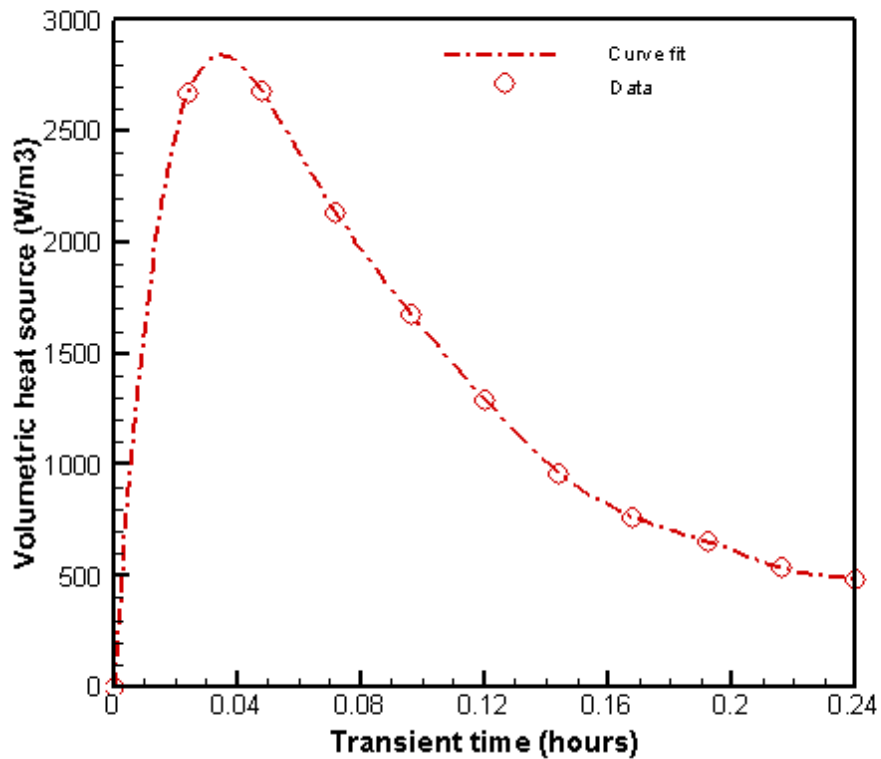
$$F = -1.25344512309040240000 \times 10^{10}$$

$$G = 9.79732902553988650000 \times 10^{10}$$

$$H = -4.09488281172600040000 \times 10^{11}$$

$$I = 8.93311908468470950000 \times 10^{11}$$

$$J = -8.00613695220408080000 \times 10^{11}$$



For time, t (hours), of $0.24 < t < 0.72$ hours,

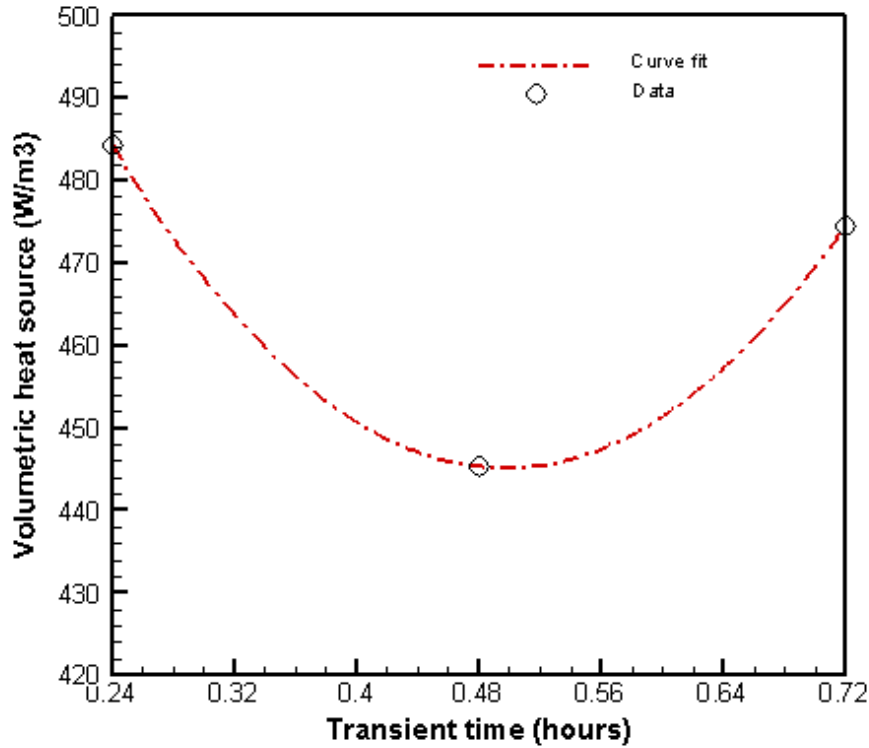
$$q''' = A + B*t + C t^2$$

where

$$A = 5.91387469886406050000 \times 10^2$$

$$B = -5.88668317582889930000 \times 10^2$$

$$C = 5.92151406914204590000 \times 10^2$$



For time, t (hours), of $0.72 < t < 12$ hours,

$$q''' = A + B*t + C t^2 + Dt^3 + Et^4 + Ft^5 + G t^6$$

where

$$A = 8.36978990287800000000 \times 10^2$$

$$B = -6.32717578411004300000 \times 10^2$$

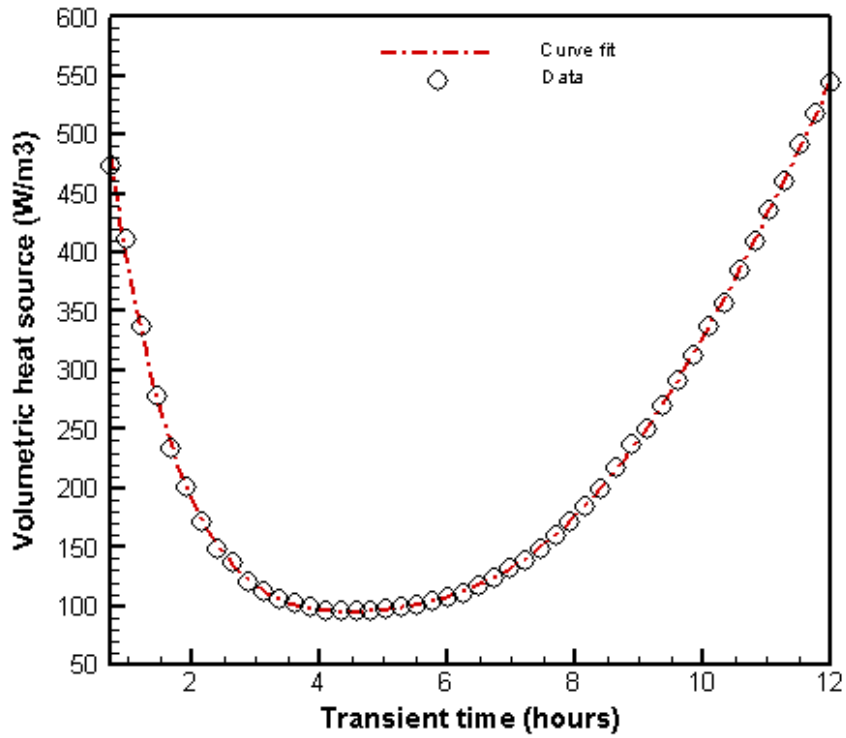
$$C = 2.22007473192730570000 \times 10^2$$

$$D = -4.10412851636717020000 \times 10^1$$

$$E = 4.15940305886652960000$$

$$F = -2.12365484046295100000 \times 10^{-1}$$

$$G = 4.30191142736251630000 \times 10^{-3}$$



For time, t (hours), of $12 < t < 19$ hours,

$$q''' = A + B*t + C t^2 + Dt^3$$

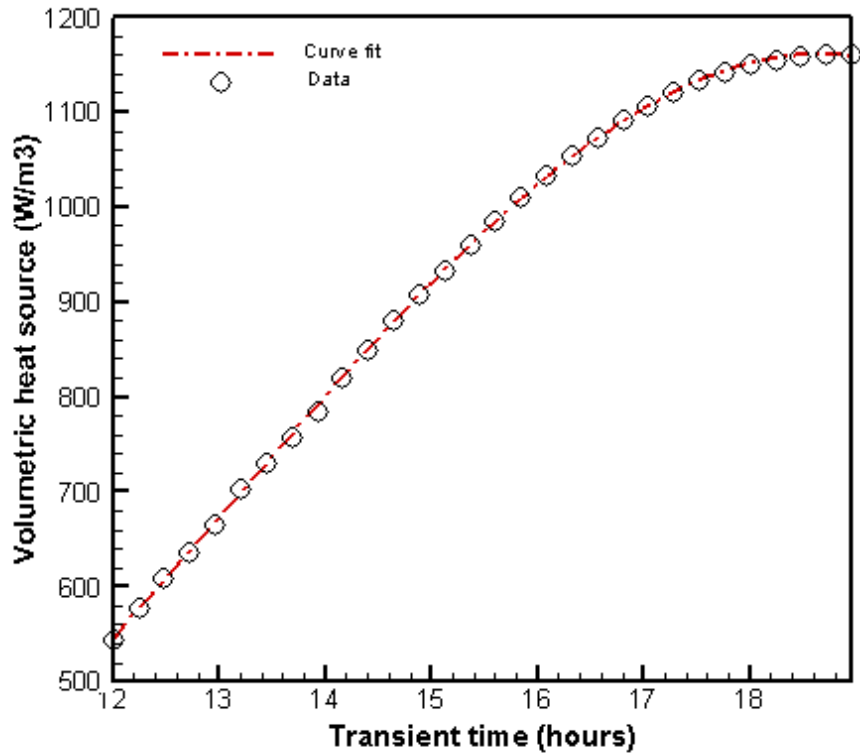
where

$$A = 2.11856848282413100000 \times 10^3$$

$$B = -5.85310747715714230000 \times 10^2$$

$$C = 5.45126997998306350000 \times 10^1$$

$$D = -1.38781058343246850000$$



For time, t (hours), of $19 < t < 101$ hours,

$$q''' = A + B*t + C t^2 + Dt^3 + Et^4 + Ft^5 + G t^6$$

where

$$A = 1.46798929537912480000 \times 10^3$$

$$B = 6.74536585645678600000 \times 10^1$$

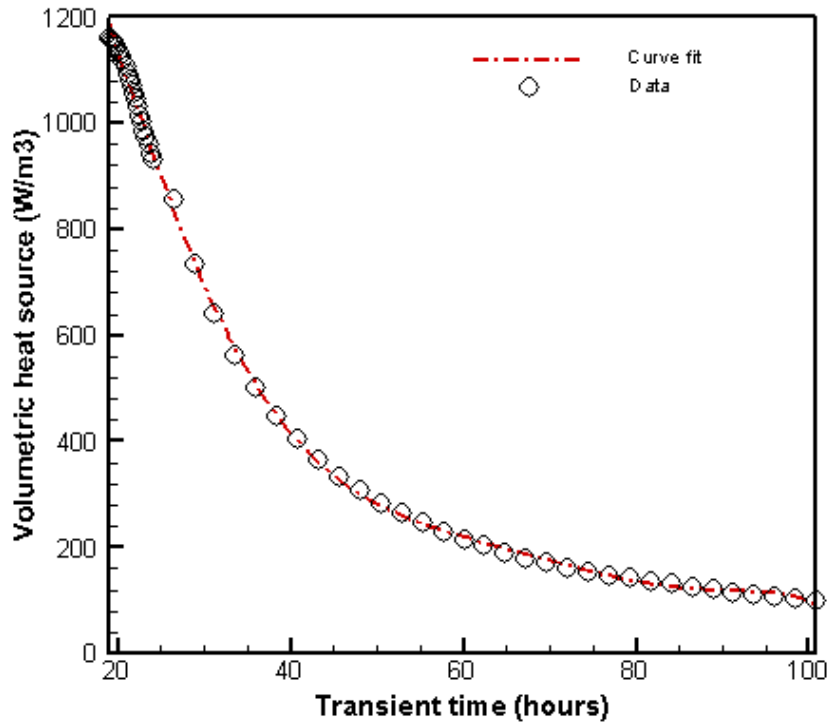
$$C = -7.82367256189775070000$$

$$D = 2.41740066120051280000 \times 10^{-1}$$

$$E = -3.48693519366358090000 \times 10^{-3}$$

$$F = 2.43804005250953660000 \times 10^{-5}$$

$$G = -6.67292127642433280000 \times 10^{-8}$$



For time t (hours) of $101 < t < 1320$ hours,

$$q''' = A + B*t + C t^2 + Dt^3 + Et^4 + Ft^5 + G t^6 + Ht^7 + It^8 + Jt^9$$

where

$$A = 4.13945191878824910000 \times 10^2$$

$$B = -5.82829436012035810000$$

$$C = 3.84926449894706780000 \times 10^{-2}$$

$$D = -1.45564940375876960000 \times 10^{-4}$$

$$E = 3.40903157334764630000 \times 10^{-7}$$

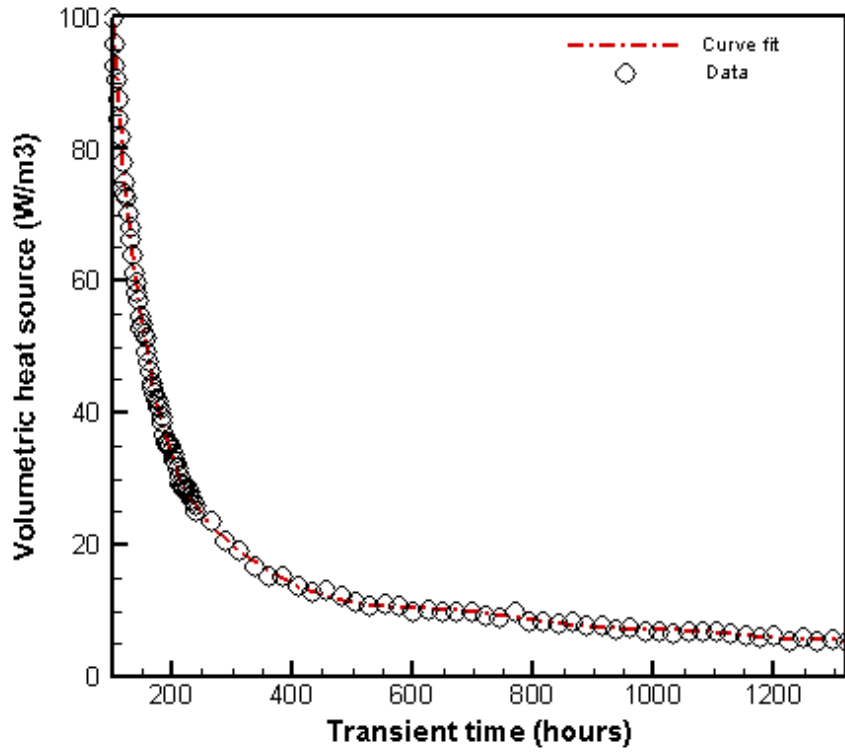
$$F = -5.10062783018528850000 \times 10^{-10}$$

$$G = 4.87733230569009760000 \times 10^{-13}$$

$$H = -2.88165150520636210000 \times 10^{-16}$$

$$I = 9.57751400690102470000 \times 10^{-20}$$

$$J = -1.36897348986712160000 \times 10^{-23}$$



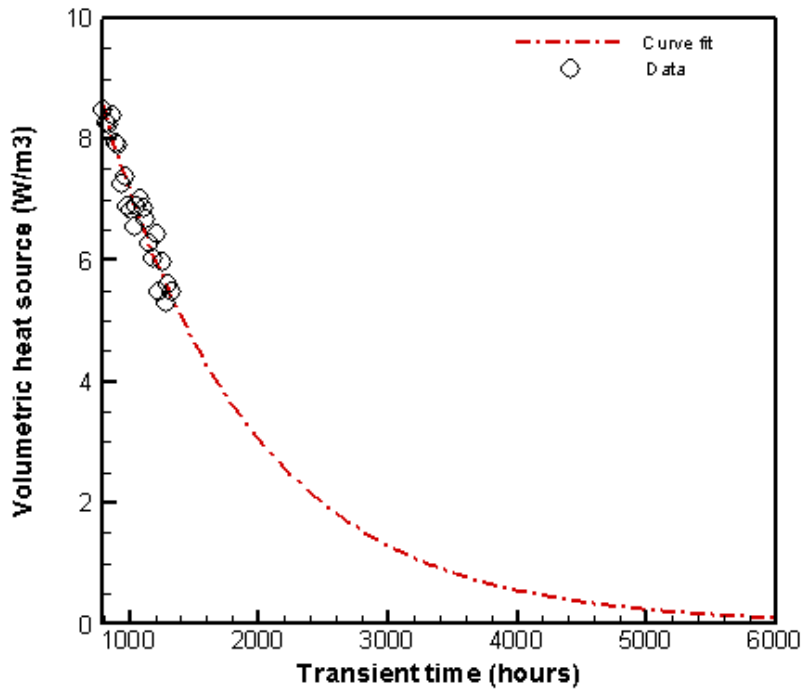
For time t (hours) $>$ 1320 hours,

$$q''' = e^{(At+B)}$$

where

$$A = -8.55474410336134050000 \times 10^{-4}$$

$$B = 2.82293843273920510000$$



A-2. Transient heat source terms for SDU6 grout region:

For time, t (hours), of $0 < t < 0.24$ hours,

$$q''' = A + Bt + C t^2 + Dt^3 + Et^4 + Ft^5 + Gt^6 + Ht^7 + It^8 + Jt^9$$

where

$$A = 0.0$$

$$B = 1.96804647032513400000 \times 10^5$$

$$C = -7.89056561184678970000 \times 10^6$$

$$D = 1.86266791019304810000 \times 10^8$$

$$E = -2.79873846123373080000 \times 10^9$$

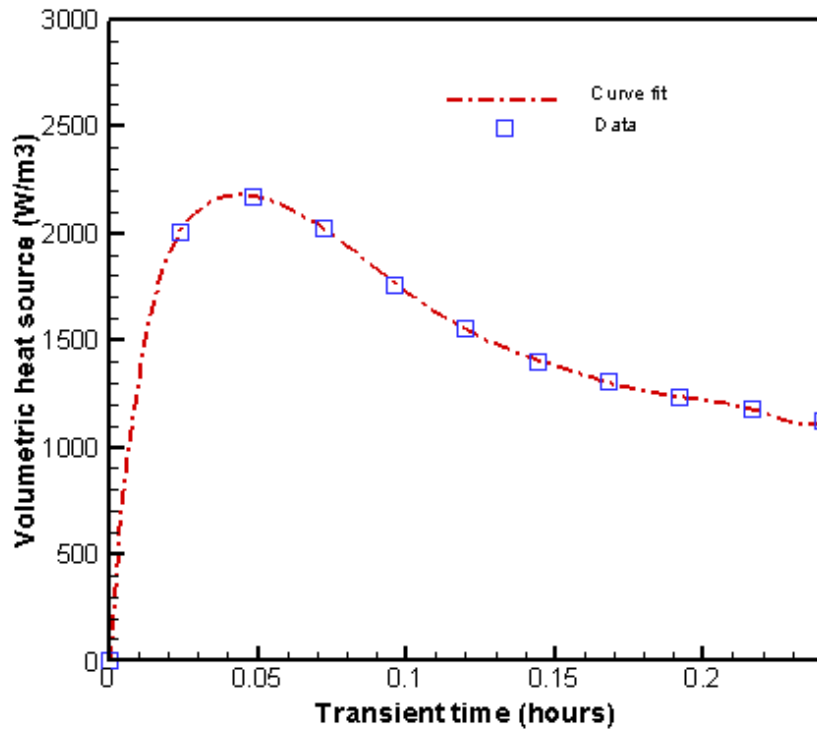
$$F = 2.67766898102183070000 \times 10^{10}$$

$$G = -1.61400863457007720000 \times 10^{11}$$

$$H = 5.91991202017225460000 \times 10^{11}$$

$$I = -1.20518532177952860000 \times 10^{12}$$

$$J = 1.04341533474120310000 \times 10^{12}$$



For time, t (hours), of $0.24 < t < 0.72$ hours,

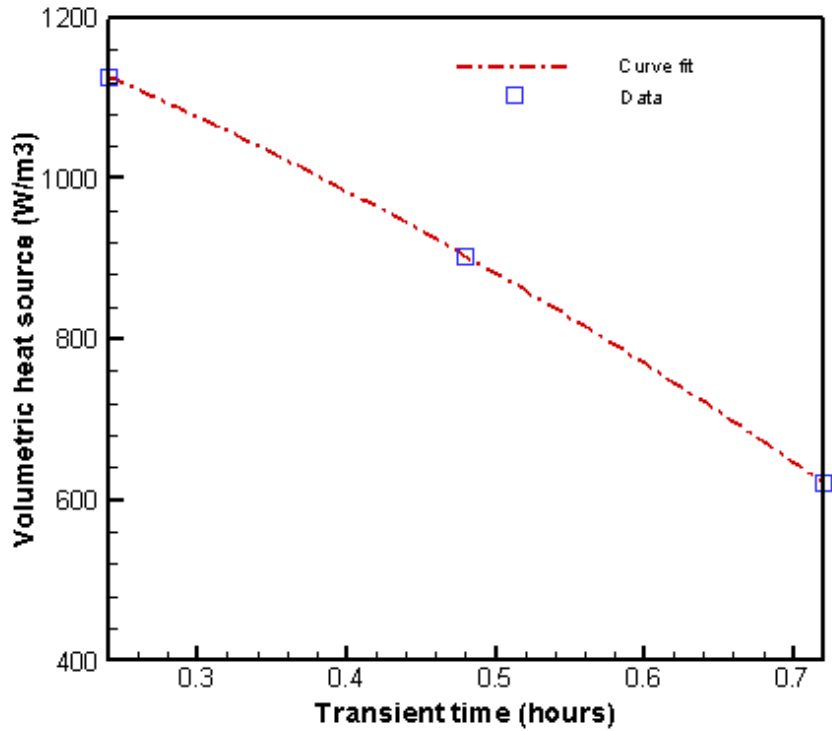
$$q''' = A + B*t + C t^2$$

where

$$A = 1.29220007001420300000 \times 10^3$$

$$B = -5.69375602903191180000 \times 10^2$$

$$C = -5.02603369444996700000 \times 10^2$$



For time, t (hours), of $0.72 < t < 12$ hours,

$$q''' = A + Bt + Ct^2 + Dt^3 + Et^4 + Ft^5 + Gt^6 + Ht^7 + It^8 + Jt^9$$

where

$$A = 2.35226497049260480000 \times 10^3$$

$$B = -4.12527877623960100000 \times 10^3$$

$$C = 3.14351130141504470000 \times 10^3$$

$$D = -1.12066789837874190000 \times 10^3$$

$$E = 1.49251843084495190000 \times 10^2$$

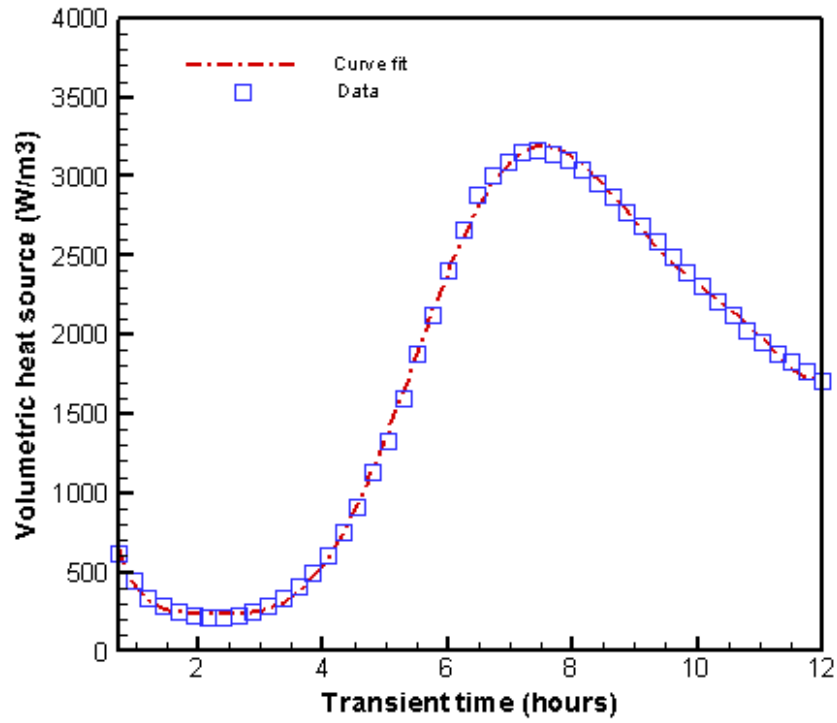
$$F = 1.58149889743340890000 \times 10^1$$

$$G = -7.35186708020694280000$$

$$H = 9.0349015856481707000 \times 10^{-1}$$

$$I = -4.94635157380416480000 \times 10^{-2}$$

$$J = 1.03683732751863100000 \times 10^{-3}$$



For time, t (hours), of $12 < t < 19$ hours,

$$q''' = A + B*t + C t^2 + D t^3$$

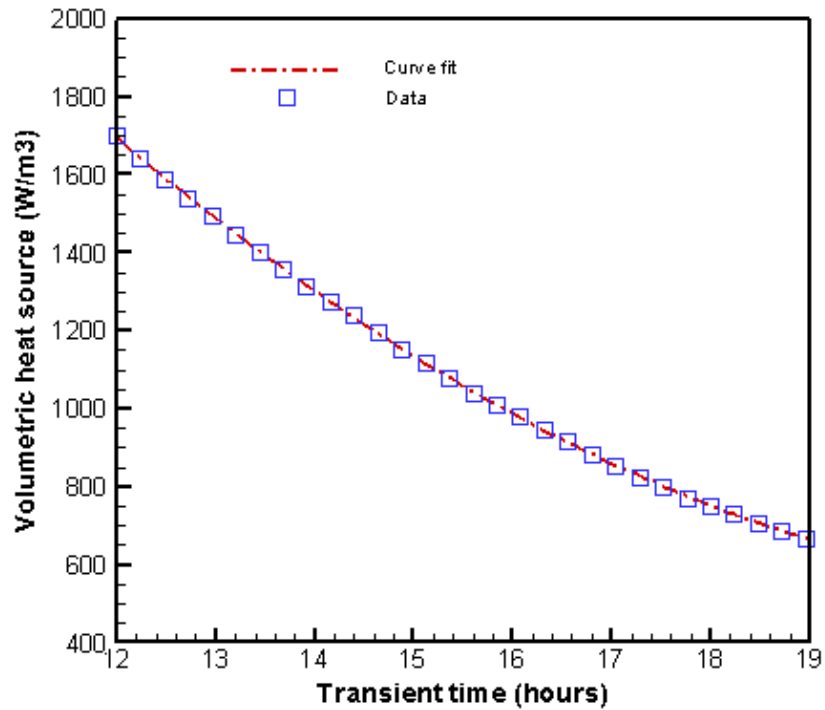
where

$$A = 5.55160746757462130000 \times 10^3$$

$$B = -4.21909722559824560000 \times 10^2$$

$$C = 7.84931128788842790000$$

$$D = 4.29340256754111930000 \times 10^{-2}$$

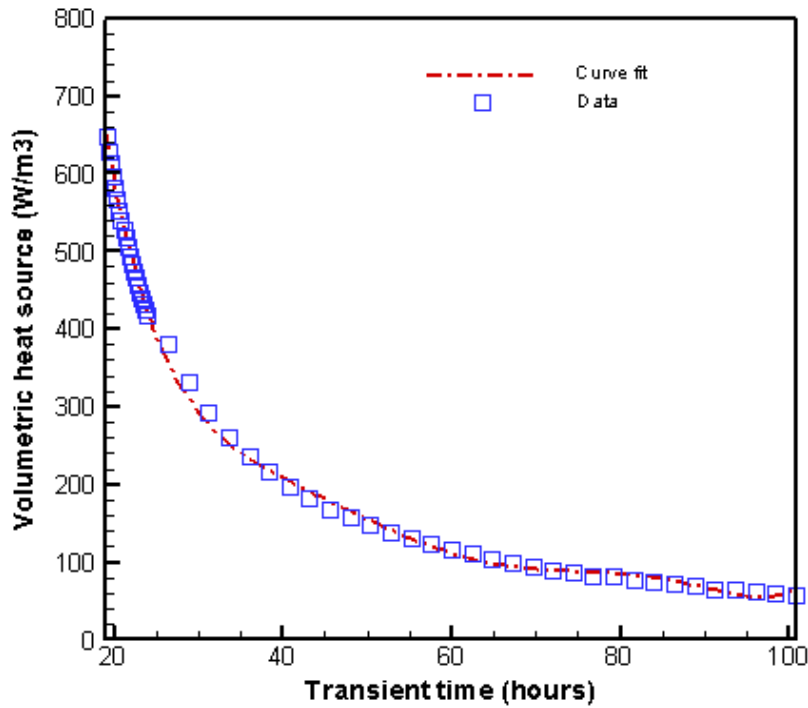


For time, t (hours), of $19 < t < 101$ hours,

$$q''' = A + B*t + C t^2 + Dt^3 + Et^4 + Ft^5 + G t^6$$

where

$$\begin{aligned} A &= 4.53332270853887440000 \times 10^3 \\ B &= -4.42287242687556100000 \times 10^2 \\ C &= 1.89816838940353460000 \times 10^1 \\ D &= -4.29973751206436270000 \times 10^{-1} \\ E &= 5.33396424970653850000 \times 10^{-3} \\ F &= -3.42287685962404290000 \times 10^{-5} \\ G &= 8.88050109119817030000 \times 10^{-8} \end{aligned}$$



For time, t (hours), of $101 < t < 1320$ hours,

$$q''' = A + B*t + C t^2 + Dt^3 + Et^4 + Ft^5 + G t^6 + Ht^7 + It^8 + Jt^9$$

where

$$A = 2.07048958358744560000 \times 10^2$$

$$B = -2.70140300079108010000$$

$$C = 1.72071893610670660000 \times 10^{-2}$$

$$D = -6.31004256380568660000 \times 10^{-5}$$

$$E = 1.43125804156685520000 \times 10^{-7}$$

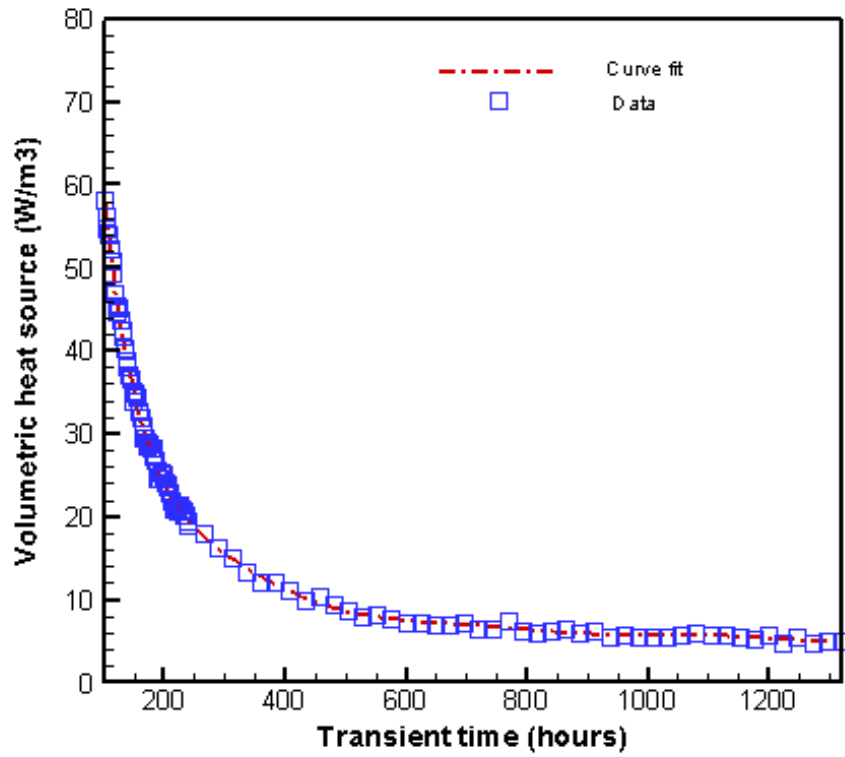
$$F = -2.07050762926181990000 \times 10^{-10}$$

$$G = 1.91213972525981850000 \times 10^{-13}$$

$$H = -1.09042564389717580000 \times 10^{-16}$$

$$I = 3.49687320769179610000 \times 10^{-20}$$

$$J = -4.82186287680667460000 \times 10^{-24}$$



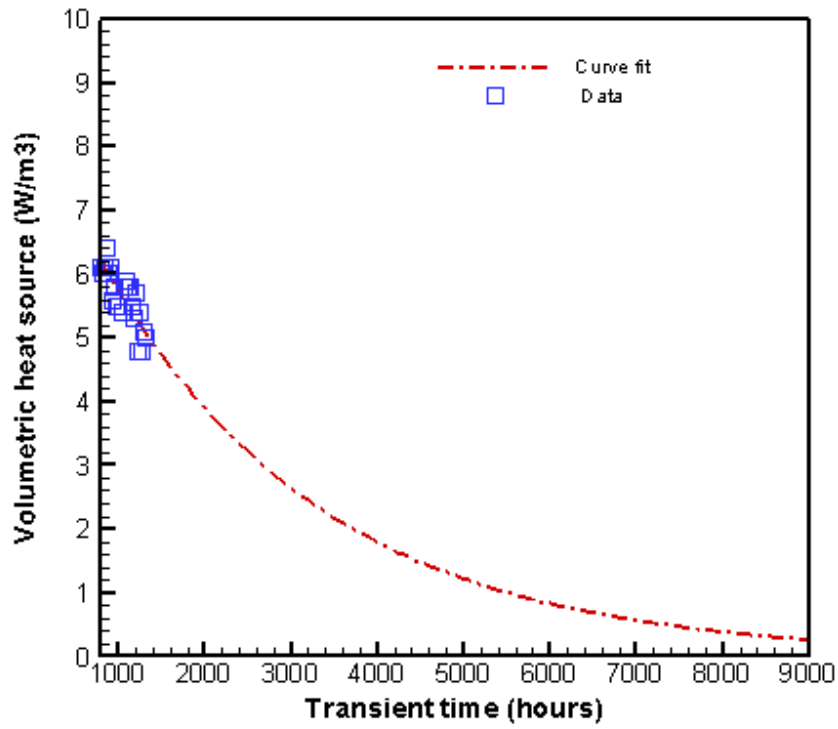
For time, t (hours), of $t > 1320$ hours,

$$q''' = e^{(At+B)}$$

where

$$A = -3.88314058068484550000 \times 10^{-4}$$

$$B = 2.13462310296217960000$$



A-3. Grout pouring schedule used for the thermal analysis of SDU facility

At transient time t = 0 hr, h = 16" = 1.333 ft (Cold cap height)									
	Start	Operation	Total time			Transient time			Model source
Date	time	hours	hours	Adding (ft)	Δh (ft)	Hours	days	h(ft)	name
8/10/2012	15:32	0.78	0.78	0.018	0.018	0.78	0.0325	1.35	grout1
		3019.18	3019.96	0.018	0	3019.96	125.8317	1.35	
12/14/2012	11:30	5.17	3025.13	0.305	0.305	3025.13	126.0471	1.66	grout2
		40.28	3065.41	0.305	0	3065.41	127.7254	1.66	
12/16/2012	8:57	7.52	3072.93	0.464	0.464	3072.93	128.0388	2.12	grout3
		41.75	3114.68	0.464	0	3114.68	129.7783	2.12	
12/18/2012	10:13	6.27	3120.95	0.376	0.376	3120.95	130.0396	2.50	grout4
		17.35	3138.3	0.376	0	3138.3	130.7625	2.50	
12/19/2012	9:15	6.85	3145.15	0.418	0.418	3145.15	131.0479	2.91	grout5
		15.73	3160.88	0.418	0	3160.88	131.7033	2.91	
12/20/2012	8:25	6.1	3166.98	0.363	0.363	3166.98	131.9575	3.28	grout6
		186.77	3353.75	0.363	0	3353.75	139.7396	3.28	
12/28/2012	9:17	6.23	3359.98	0.37	0.37	3359.98	139.9992	3.65	grout7
		1840.52	5200.5	0.37	0	5200.5	216.6875	3.65	
3/15/2013	8:02	8.82	5209.32	0.5	0.5	5209.32	217.055	4.15	grout8
		64.02	5273.34	0.5	0	5273.34	219.7225	4.15	
3/18/2013	8:52	8.02	5281.36	0.497	0.497	5281.36	220.0567	4.64	grout9
		15.83	5297.19	0.497	0	5297.19	220.7163	4.64	
3/19/2013	8:43	8.18	5305.37	0.509	0.509	5305.37	221.0571	5.15	grout10
		15.07	5320.44	0.509	0	5320.44	221.685	5.15	
3/20/2013	7:58	8.93	5329.37	0.535	0.535	5329.37	222.0571	5.69	grout11
		280	5609.37	0.535	0	5609.37	233.7238	5.69	
4/1/2013	8:54	7.67	5617.04	0.474	0.474	5617.04	234.0433	6.16	grout12
		15.85	5632.89	0.474	0	5632.89	234.7038	6.16	
4/2/2013	8:25	8.28	5641.17	0.515	0.515	5641.17	235.0488	6.68	grout13
		39.53	5680.7	0.515	0	5680.7	236.6958	6.68	
4/4/2013	8:14	8.47	5689.17	0.508	0.508	5689.17	237.0488	7.19	grout14
		16	5705.17	0.508	0	5705.17	237.7154	7.19	
4/5/2013	8:42	7.85	5713.02	0.486	0.486	5713.02	238.0425	7.67	grout15
		15.13	5728.15	0.486	0	5728.15	238.6729	7.67	
4/6/2013	7:41	6.63	5734.78	0.393	0.393	5734.78	238.9492	8.06	grout16
		186.22	5921	0.393	0	5921	246.7083	8.06	
4/14/2013	8:32	7.97	5928.97	0.491	0.491	5928.97	247.0404	8.56	grout17
		15.68	5944.65	0.491	0	5944.65	247.6938	8.56	

4/15/2013	8:11	8.02	5952.67	0.461	0.461	5952.67	248.0279	9.02	grout18
		16.3	5968.97	0.461	0	5968.97	248.7071	9.02	
Date	time	hours	hours	Adding (ft)	Δh (ft)	Hours	days	h(ft)	name
4/16/2013	8:30	8.13	5977.1	0.495	0.495	5977.1	249.0458	9.51	grout19
		15.32	5992.42	0.495	0	5992.42	249.6842	9.51	
4/17/2013	7:57	8.82	6001.24	0.526	0.526	6001.24	250.0517	10.04	grout20
		39.28	6040.52	0.526	0	6040.52	251.6883	10.04	
4/19/2013	8:03	8.32	6048.84	0.487	0.487	6048.84	252.035	10.52	grout21
		40.13	6088.97	0.487	0	6088.97	253.7071	10.52	
4/21/2013	8:30	1.27	6090.24	0.044	0.044	6090.24	253.76	10.57	grout22
		95.18	6185.42	0.044	0	6185.42	257.7258	10.57	
4/25/2013	9:27	1.43	6186.85	0.052	0.052	6186.85	257.7854	10.62	grout23
		1462.13	7648.98	0.052	0	7648.98	318.7075	10.62	
6/25/2013	9:01	6.33	7655.31	0.377	0.377	7655.31	318.9713	11.00	grout24
		17.82	7673.13	0.377	0	7673.13	319.7138	11.00	
6/26/2013	9:10	6.35	7679.48	0.382	0.382	7679.48	319.9783	11.38	grout25
		858.78	8538.26	0.382	0	8538.26	355.7608	11.38	
8/1/2013	10:18	6.08	8544.34	0.359	0.359	8544.34	356.0142	11.74	grout26
		40.65	8584.99	0.359	0	8584.99	357.7079	11.74	
8/3/2013	9:02	7.37	8592.36	0.448	0.448	8592.36	358.015	12.19	grout27
		17.77	8610.13	0.448	0	8610.13	358.7554	12.19	
8/4/2013	10:10	6.48	8616.61	0.391	0.391	8616.61	359.0254	12.58	grout28
		15.72	8632.33	0.391	0	8632.33	359.6804	12.58	
8/5/2013	8:22	8.25	8640.58	0.508	0.508	8640.58	360.0242	13.09	grout29
		16.13	8656.71	0.508	0	8656.71	360.6963	13.09	
8/6/2013	8:45	7.68	8664.39	0.471	0.471	8664.39	361.0163	13.56	grout30
		16	8680.39	0.471	0	8680.39	361.6829	13.56	
8/7/2013	8:23	8.12	8688.51	0.495	0.495	8688.51	362.0213	14.05	grout31
		16.25	8704.76	0.495	0	8704.76	362.6983	14.05	
8/8/2013	8:45	7.52	8712.28	0.463	0.463	8712.28	363.0117	14.51	grout32
		16.78	8729.06	0.463	0	8729.06	363.7108	14.51	
8/9/2013	9:03	7.5	8736.56	0.462	0.462	8736.56	364.0233	14.98	grout33
		15.72	8752.28	0.462	0	8752.28	364.6783	14.98	
8/10/2013	8:16	8.25	8760.53	0.508	0.508	8760.53	365.0221	15.48	grout34
		16.1	8776.63	0.508	0	8776.63	365.6929	15.48	
8/11/2013	8:37	8.2	8784.83	0.509	0.509	8784.83	366.0346	15.99	grout35
		18.28	8803.11	0.509	0	8803.11	366.7963	15.99	
8/12/2013	11:06	4.93	8808.04	0.286	0.286	8808.04	367.0017	16.28	grout36
		40.58	8848.62	0.286	0	8848.62	368.6925	16.28	
8/14/2013	8:37	8.1	8856.72	0.493	0.493	8856.72	369.03	16.77	grout37
		39.63	8896.35	0.493	0	8896.35	370.6813	16.77	

8/16/2013	8:21	8.12	8904.47	0.486	0.486	8904.47	371.0196	17.26	grout38
		2801.43	11705.9	0.486	0	11705.9	487.7458	17.26	
Date	time	hours	hours	Adding (ft)	Δh (ft)	Hours	days	h(ft)	name
12/11/2013	9:54	5.27	11711.17	0.286	0.286	11711.17	487.9654	17.54	grout39
		113.8	11824.97	0.286	0	11824.97	492.7071	17.54	
12/16/2013	8:58	4.03	11829	0.23	0.23	11829	492.875	17.77	grout40
		67.35	11896.35	0.23	0	11896.35	495.6813	17.77	
12/19/2013	8:21	0.68	11897.03	0.002	0.002	11897.03	495.7096	17.78	neglected
		1.67	11898.7	0.002	0	11898.7	495.7792	17.78	
12/19/2013	10:42	0.55	11899.25	0	0	11899.25	495.8021	17.78	
		3622.9	15522.15	0	0	15522.15	646.7563	17.78	
5/19/2014	10:09	4.8	15526.95	0.269	0.269	15526.95	646.9563	18.05	grout41
		18.02	15544.97	0.269	0	15544.97	647.7071	18.05	
5/20/2014	8:58	5.95	15550.92	0.33	0.33	15550.92	647.955	18.38	grout42
		18.63	15569.55	0.33	0	15569.55	648.7313	18.38	
5/21/2014	9:33	3.22	15572.77	0.206	0.206	15572.77	648.8654	18.58	grout43
		140.75	15713.52	0.206	0	15713.52	654.73	18.58	
5/27/2014	9:31	0.63	15714.15	0	0	15714.15	654.7563	18.58	
		22.53	15736.68	0	0	15736.68	655.695	18.58	
5/28/2014	8:41	6.27	15742.95	0.384	0.384	15742.95	655.9563	18.97	grout44
		17.95	15760.9	0.384	0	15760.9	656.7042	18.97	
5/29/2014	8:54	5.97	15766.87	0.36	0.36	15766.87	656.9529	19.33	grout45
		114.8	15881.67	0.36	0	15881.67	661.7363	19.33	
6/3/2014	9:40	5.25	15886.92	0.317	0.317	15886.92	661.955	19.64	grout46
		42	15928.92	0.317	0	15928.92	663.705	19.64	
6/5/2014	8:55	6.02	15934.94	0.334	0.334	15934.94	663.9558	19.98	grout47
		89.68	16024.62	0.334	0	16024.62	667.6925	19.98	
6/9/2014	8:37	6.32	16030.94	0.385	0.385	16030.94	667.9558	20.36	grout48
		17.8	16048.74	0.385	0	16048.74	668.6975	20.36	
6/10/2014	8:44	6.2	16054.94	0.371	0.371	16054.94	668.9558	20.73	grout49
		17.37	16072.31	0.371	0	16072.31	669.6796	20.73	
6/11/2014	8:18	3.98	16076.29	0.197	0.197	16076.29	669.8454	20.93	grout50
	12:17	(239 minutes poured, = 3.98 hours operated)							

A-4. Grout pouring schedule used for the thermal analysis of SDU 6

Based on 150 gpm grout pour, 295 hours pour, 1118 hours break					
Operational time			Grout height	Grout aging	Model source
Date	hours	days	feet	(hours)	name
1/1/2017	0	0.0	0	6	grout 1
	12	0.5	0.1307	6	grout 2
1/2/2017	24	1.0	0.2614	6	grout 3
	36	1.5	0.3921	6	grout 4
1/3/2017	48	2.0	0.5228	6	grout 5
	60	2.5	0.6535	6	grout 6
1/4/2017	72	3.0	0.7842	6	grout 7
	84	3.5	0.9149	6	grout 8
1/5/2017	96	4.0	1.0456	6	grout 9
	108	4.5	1.1763	6	grout 10
1/6/2017	120	5.0	1.307	6	grout 11
	132	5.5	1.4377	6	grout 12
1/7/2017	144	6.0	1.5684	6	grout 13
	156	6.5	1.6991	6	grout 14
1/8/2017	168	7.0	1.8298	6	grout 15
	180	7.5	1.9605	6	grout 16
1/9/2017	192	8.0	2.0912	6	grout 17
	204	8.5	2.2219	6	grout 18
1/10/2017	216	9.0	2.3526	6	grout 19
	228	9.5	2.4833	6	grout 20
1/11/2017	240	10.0	2.614	6	grout 21
	252	10.5	2.7447	6	grout 22
1/12/2017	264	11.0	2.8754	6	grout 23
	276	11.5	3.0061	6	grout 24
1/13/2017	288	12.0	3.1368	3.5	grout 25
End pour	295	12.3	3.213	147.5	End pour
1/14/2017	312	13.0	3.213		Idling
1/15/2017	336	14.0	3.213		Idling
1/16/2017	360	15.0	3.213		Idling
2/25/2017	1320	55.0	3.213		Idling
2/26/2017	1344	56.0	3.213		Idling

2/27/2017	1368	57.0	3.213		Idling
2/28/2017	1392	58.0	3.213		Idling
2/28/2017	1413	58.9	3.213	7.5	grout26 start
Date	hours	days	feet	(hours)	name
3/1/2017	1416	59.0			
	1428	59.5	3.3764	6	grout27
3/2/2017	1440	60.0	3.5071	6	grout28
	1452	60.5	3.6378	6	grout29
3/3/2017	1464	61.0	3.7685	6	grout30
	1476	61.5	3.8992	6	grout31
3/4/2017	1488	62.0	4.0299	6	grout32
	1500	62.5	4.1606	6	grout33
3/5/2017	1512	63.0	4.2913	6	grout34
	1524	63.5	4.422	6	grout35
3/6/2017	1536	64.0	4.5527	6	grout36
	1548	64.5	4.6834	6	grout37
3/7/2017	1560	65.0	4.8141	6	grout38
	1572	65.5	4.9448	6	grout39
3/8/2017	1584	66.0	5.0755	6	grout40
	1596	66.5	5.2062	6	grout41
3/9/2017	1608	67.0	5.3369	6	grout42
	1620	67.5	5.4676	6	grout43
3/10/2017	1632	68.0	5.5983	6	grout44
	1644	68.5	5.729	6	grout45
3/11/2017	1656	69.0	5.8597	6	grout46
	1668	69.5	5.9904	6	grout47
3/12/2017	1680	70.0	6.1211	6	grout48
3/12/2017	1692	70.5	6.2518	8	grout49
3/13/2017	1704	71.0			
	1708	71.2	6.4261	147.5	End pour
3/14/2017	1728	72.0	6.4261		Idling
3/15/2017	1752	73.0	6.4261		Idling
3/16/2017	1776	74.0	6.4261		Idling
4/26/2017	2760	115.0	6.4261		Idling
4/27/2017	2784	116.0	6.4261		Idling
4/28/2017	2808	117.0	6.4261		Idling
	2826	117.8	6.4261	3	grout50
4/29/2017	2832	118.0	6.4914	6	grout51
	2844	118.5	6.6221	6	grout52
4/30/2017	2856	119.0	6.7528	6	grout53

	2868	119.5	6.8835	6	grout54
5/1/2017	2880	120.0	7.0142	6	grout55
	2892	120.5	7.1449	6	grout56

Date	hours	days	feet	(hours)	name
5/2/2017	2904	121.0	7.2756	6	grout57
	2916	121.5	7.4063	6	grout58
5/3/2017	2928	122.0	7.537	6	grout59
	2940	122.5	7.6677	6	grout60
5/4/2017	2952	123.0	7.7984	6	grout61
	2964	123.5	7.9291	6	grout62
5/5/2017	2976	124.0	8.0598	6	grout63
	2988	124.5	8.1905	6	grout64
5/6/2017	3000	125.0	8.3212	6	grout65
	3012	125.5	8.4519	6	grout66
5/7/2017	3024	126.0	8.5826	6	grout67
	3036	126.5	8.7133	6	grout68
5/8/2017	3048	127.0	8.844	6	grout69
	3060	127.5	8.9747	6	grout70
5/9/2017	3072	128.0	9.1054	6	grout71
	3084	128.5	9.2361	6	grout72
5/10/2017	3096	129.0	9.3668	6	grout73
	3108	129.5	9.4975	6.5	grout74
5/11/2017	3120	130.0			
	3121	130.0	9.6391	147.5	End pour
5/12/2017	3144	131.0	9.6391		Idling
5/13/2017	3168	132.0	9.6391		Idling
5/14/2017	3192	133.0	9.6391		Idling
5/15/2017	3216	134.0	9.6391		Idling
5/16/2017	3240	135.0	9.6391		Idling
6/23/2017	4152	173.0	9.6391		Idling
6/24/2017	4176	174.0	9.6391		Idling
6/25/2017	4200	175.0	9.6391		Idling
6/26/2017	4224	176.0	9.6391		Idling
	4239	176.6	9.6391	4.5	grout 75
6/27/2017	4248	177.0	9.7371	6	grout 76
	4260	177.5	9.8678	6	grout 77
6/28/2017	4272	178.0	9.9985	6	grout 78
	4284	178.5	10.1292	6	grout 79
6/29/2017	4296	179.0	10.2599	6	grout 80
	4308	179.5	10.3906	6	grout 81
6/30/2017	4320	180.0	10.5213	6	grout 82
	4332	180.5	10.652	6	grout 83
7/1/2017	4344	181.0	10.7827	6	grout 84

Date	hours	days	feet	(hours)	name
	4356	181.5	10.9134	6	grout 85
7/2/2017	4368	182.0	11.0441	6	grout 86
	4380	182.5	11.1748	6	grout 87
7/3/2017	4392	183.0	11.3055	6	grout 88
	4404	183.5	11.4362	6	grout 89
7/4/2017	4416	184.0	11.5669	6	grout 90
	4428	184.5	11.6976	6	grout 91
7/5/2017	4440	185.0	11.8283	6	grout 92
	4452	185.5	11.959	6	grout 93
7/6/2017	4464	186.0	12.0897	6	grout 94
	4476	186.5	12.2204	6	grout 95
7/7/2017	4488	187.0	12.3511	6	grout 96
	4500	187.5	12.4818	6	grout 97
7/8/2017	4512	188.0	12.6125	6	grout 98
	4524	188.5	12.7432	5	grout 99
7/8/2017	4534	188.9	12.8521	147.5	End pour
7/9/2017	4536	189.0	12.8521		Idling
7/10/2017	4560	190.0	12.8521		Idling
7/11/2017	4584	191.0	12.8521		Idling
7/12/2017	4608	192.0	12.8521		Idling
7/13/2017	4632	193.0	12.8521		Idling
8/20/2017	5544	231.0	12.8521		Idling
8/21/2017	5568	232.0	12.8521		Idling
8/22/2017	5592	233.0	12.8521		Idling
8/23/2017	5616	234.0	12.8521		Idling
8/24/2017	5640	235.0	12.8521		Idling
	5652	235.5	12.8521	6	grout100
8/25/2017	5664	236.0	12.9828	6	grout101
	5676	236.5	13.1135	6	grout102
8/26/2017	5688	237.0	13.2442	6	grout103
	5700	237.5	13.3749	6	grout104
8/27/2017	5712	238.0	13.5056	6	grout105
	5724	238.5	13.6363	6	grout106
8/28/2017	5736	239.0	13.767	6	grout107
	5748	239.5	13.8977	6	grout108
8/29/2017	5760	240.0	14.0284	6	grout109
	5772	240.5	14.1591	6	grout110
8/30/2017	5784	241.0	14.2898	6	grout111
	5796	241.5	14.4205	6	grout112

Date	hours	days	feet	(hours)	name
8/31/2017	5808	242.0	14.5512	6	grout113
	5820	242.5	14.6819	6	grout114
9/1/2017	5832	243.0	14.8126	6	grout115
	5844	243.5	14.9433	6	grout116
9/2/2017	5856	244.0	15.074	6	grout117
	5868	244.5	15.2047	6	grout118
9/3/2017	5880	245.0	15.3354	6	grout119
	5892	245.5	15.4661	6	grout120
9/4/2017	5904	246.0	15.5968	6	grout121
	5916	246.5	15.7275	6	grout122
9/5/2017	5928	247.0	15.8582	6	grout123
	5940	247.5	15.9889	3.5	grout124
	5947	247.8	16.0652	147.5	End pour
9/6/2017	5952	248.0	16.0652		Idling
9/7/2017	5976	249.0	16.0652		Idling
9/8/2017	6000	250.0	16.0652		Idling
9/9/2017	6024	251.0	16.0652		Idling
9/10/2017	6048	252.0	16.0652		Idling
10/19/2017	6984	291.0	16.0652		Idling
10/20/2017	7008	292.0	16.0652		Idling
10/21/2017	7032	293.0	16.0652		Idling
10/22/2017	7056	294.0	16.0652		Idling
	7065	294.4	16.0652	7.5	grout125
	7077	294.9	16.1959		
10/23/2017	7080	295.0	16.2286	6	grout126
	7092	295.5	16.3593	6	grout127
10/24/2017	7104	296.0	16.49	6	grout128
	7116	296.5	16.6207	6	grout129
10/25/2017	7128	297.0	16.7514	6	grout130
	7140	297.5	16.8821	6	grout131
10/26/2017	7152	298.0	17.0128	6	grout132
	7164	298.5	17.1435	6	grout133
10/27/2017	7176	299.0	17.2742	6	grout134
	7188	299.5	17.4049	6	grout135
10/28/2017	7200	300.0	17.5356	6	grout136
	7212	300.5	17.6663	6	grout137
10/29/2017	7224	301.0	17.797	6	grout138
	7236	301.5	17.9277	6	grout139
10/30/2017	7248	302.0	18.0584	6	grout140

Date	hours	days	feet	(hours)	name
	7260	302.5	18.1891	6	grout141
10/31/2017	7272	303.0	18.3198	6	grout142
	7284	303.5	18.4505	6	grout143
11/1/2017	7296	304.0	18.5812	6	grout144
	7308	304.5	18.7119	6	grout145
11/2/2017	7320	305.0	18.8426	6	grout146
	7332	305.5	18.9733	6	grout147
11/3/2017	7344	306.0	19.104	8	grout148
	7356	306.5	19.2347		
	7360	306.7	19.2783	147.5	End pour
11/4/2017	7368	307.0	19.2783		Idling
11/5/2017	7392	308.0	19.2783		Idling
11/6/2017	7416	309.0	19.2783		Idling
11/7/2017	7440	310.0	19.2783		Idling
12/16/2017	8376	349.0	19.2783		Idling
12/17/2017	8400	350.0	19.2783		Idling
12/18/2017	8424	351.0	19.2783		Idling
12/19/2017	8448	352.0	19.2783		Idling
12/20/2017	8472	353.0	19.2783		Idling
	8478	353.3	19.2783	6	grout149
	8490	353.8	19.409	3	grout150
12/21/2017	8496	354.0	19.4743	6	grout151
	8508	354.5	19.605	6	grout152
12/22/2017	8520	355.0	19.7357	6	grout153
	8532	355.5	19.8664	6	grout154
12/23/2017	8544	356.0	19.9971	6	grout155
	8556	356.5	20.1278	6	grout156
12/24/2017	8568	357.0	20.2585	6	grout157
	8580	357.5	20.3892	6	grout158
12/25/2017	8592	358.0	20.5199	6	grout159
	8604	358.5	20.6506	6	grout160
12/26/2017	8616	359.0	20.7813	6	grout161
	8628	359.5	20.912	6	grout162
12/27/2017	8640	360.0	21.0427	6	grout163
	8652	360.5	21.1734	6	grout164
12/28/2017	8664	361.0	21.3041	6	grout165
	8676	361.5	21.4348	6	grout166
12/29/2017	8688	362.0	21.5655	6	grout167
	8700	362.5	21.6962	6	grout168

Date	hours	days	feet	(hours)	name
12/30/2017	8712	363.0	21.8269	6	grout169
	8724	363.5	21.9576	6	grout170
12/31/2017	8736	364.0	22.0883	6	grout171
	8748	364.5	22.219	6	grout172
1/1/2018	8760	365.0	22.3497	6.5	grout173
	8773	365.5	22.4913		
				147.5	End pour

Appendix B. Computer Input Files for Ambient Temperature and Hydration Heat Source

The pdf files for the computer input files will be distributed separately.

Distribution:

timothy.brown@srnl.doe.gov
alex.cozzi@srnl.doe.gov
david.crowley@srnl.doe.gov
a.fellinger@srnl.doe.gov
samuel.fink@srnl.doe.gov
nancy.halverson@srnl.doe.gov
connie.herman@srnl.doe.gov
Matthew.Kesterson@srnl.doe.gov
john.mayer@srnl.doe.gov
Gregg.Morgan@srnl.doe.gov
frank.pennebaker@srnl.doe.gov
luke.reid@srnl.doe.gov
Boyd.Wiedenman@srnl.doe.gov

patricia.suggs@srs.gov

Richard.Edwards@srs.gov
eric.freed@srs.gov
Vijay.Jain@srs.gov
kent.rosenberger@srs.gov
steven.thomas@srs.gov
Records Administration (EDWS)